Component separation for CMB B-mode satellite missions

Mathieu Remazeilles

The University of Manchester

Rencontres de Moriond
La Thuile, 17-24 March 2018

Primordial CMB B-mode power spectrum

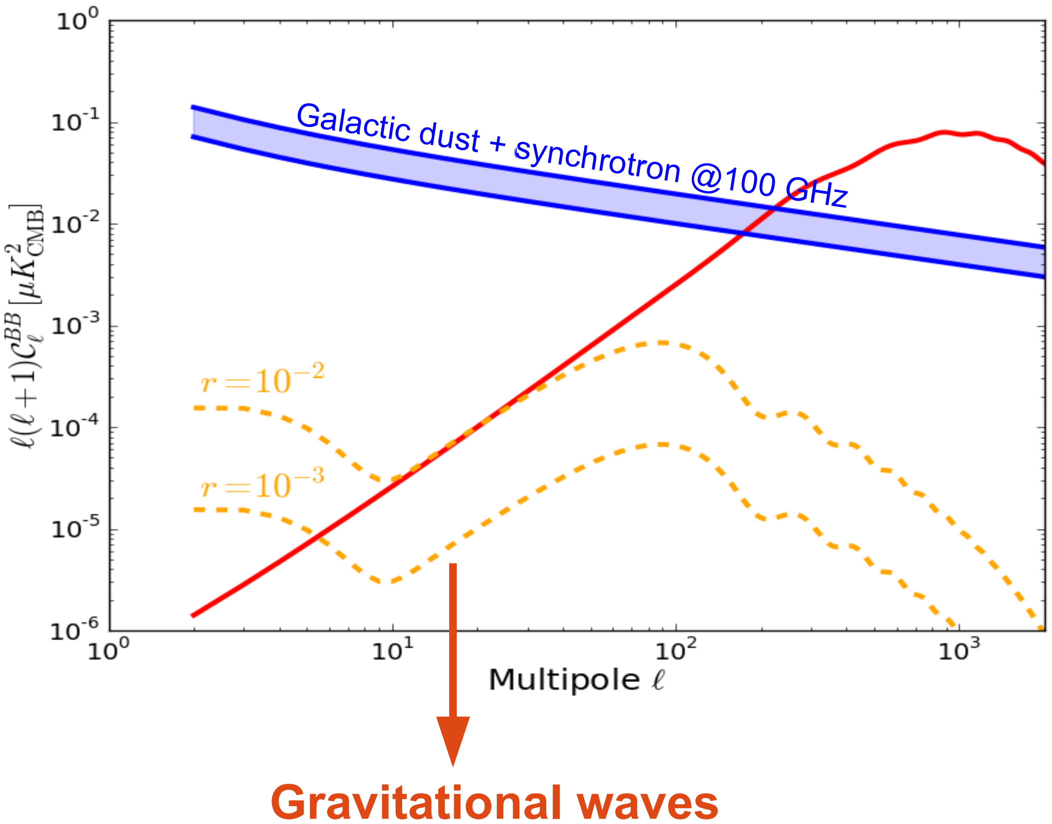

- **Large-scale primordial CMB B-mode polarization:**
  signature of primordial gravitational waves of quantum origin

- **Amplitude of primordial CMB B-modes (tensor-to-scalar ratio):**
  relates to the energy scale of inflation: **$r = 0.008 \times (E_{inflation} / 10^{16}\ \mathrm{GeV})^4$**

Primordial CMB B-mode power spectrum

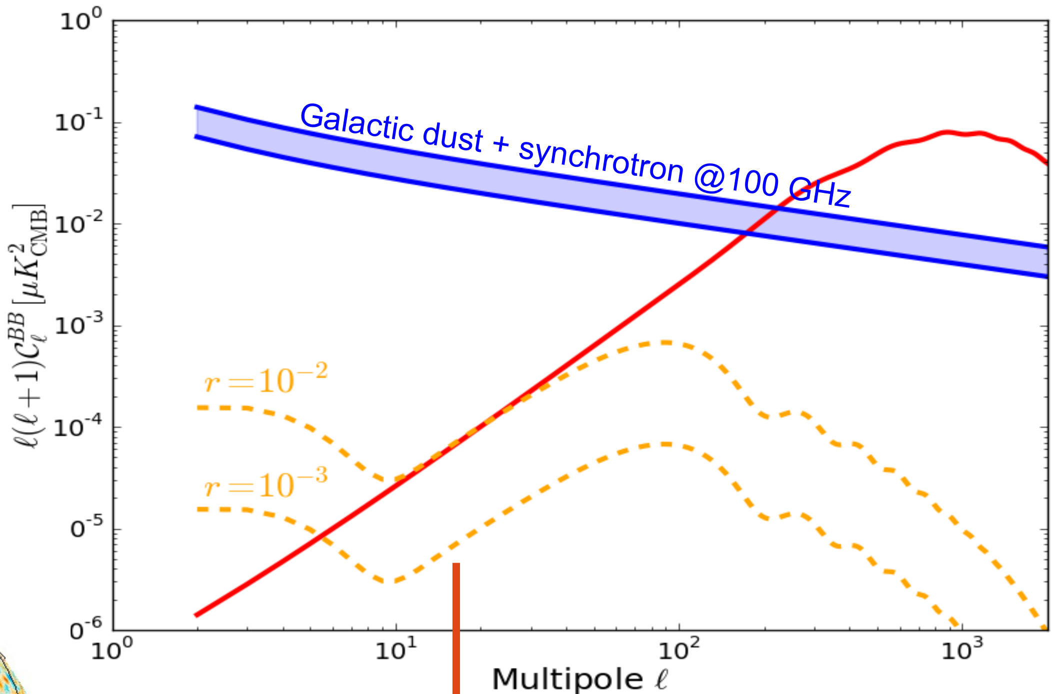

Gravitational waves

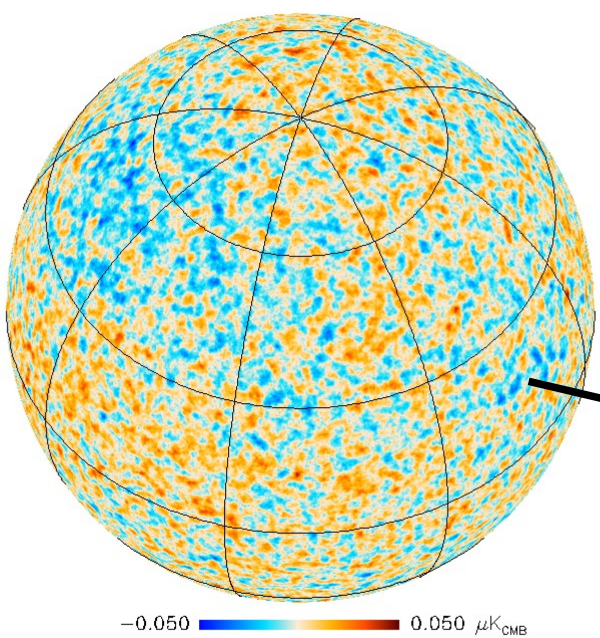

50 nK r.m.s. fluctuations!

Primordial CMB B-mode power spectrum

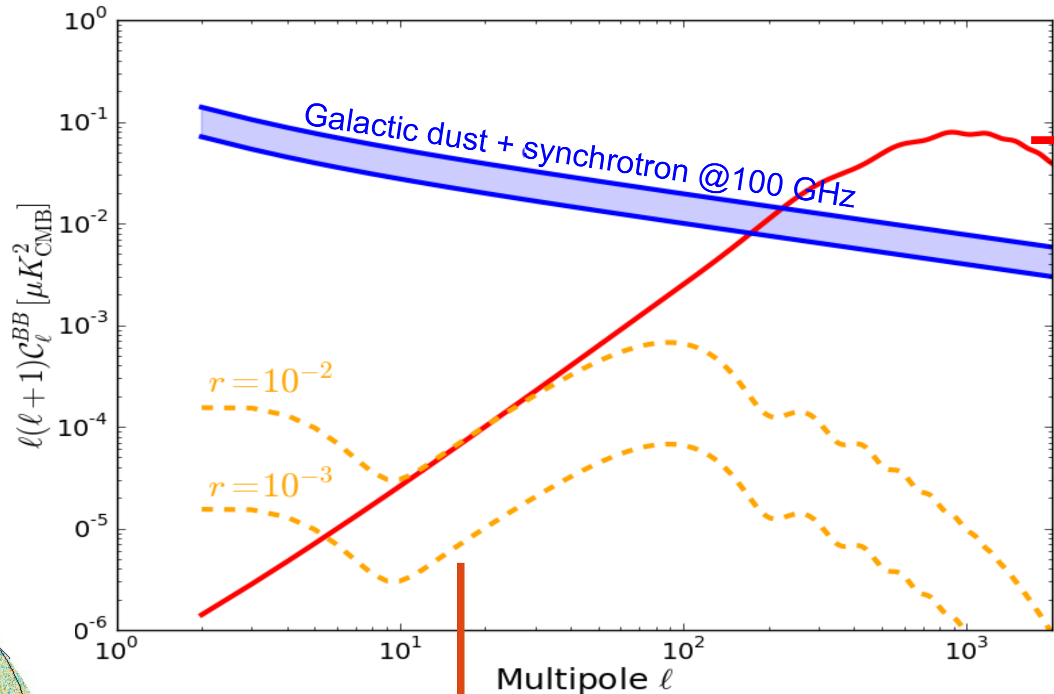

Gravitational lensing

Gravitational waves

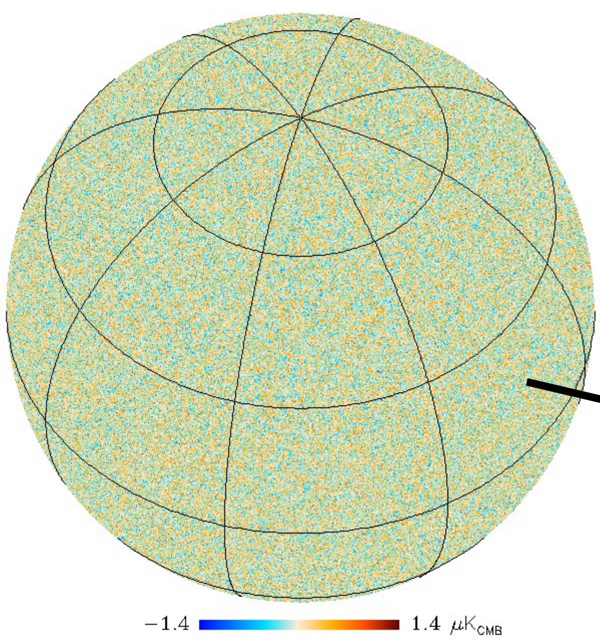

Gravitational lensing by LSS transforms CMB E-modes into spurious B-modes!

Primordial CMB B-mode power spectrum

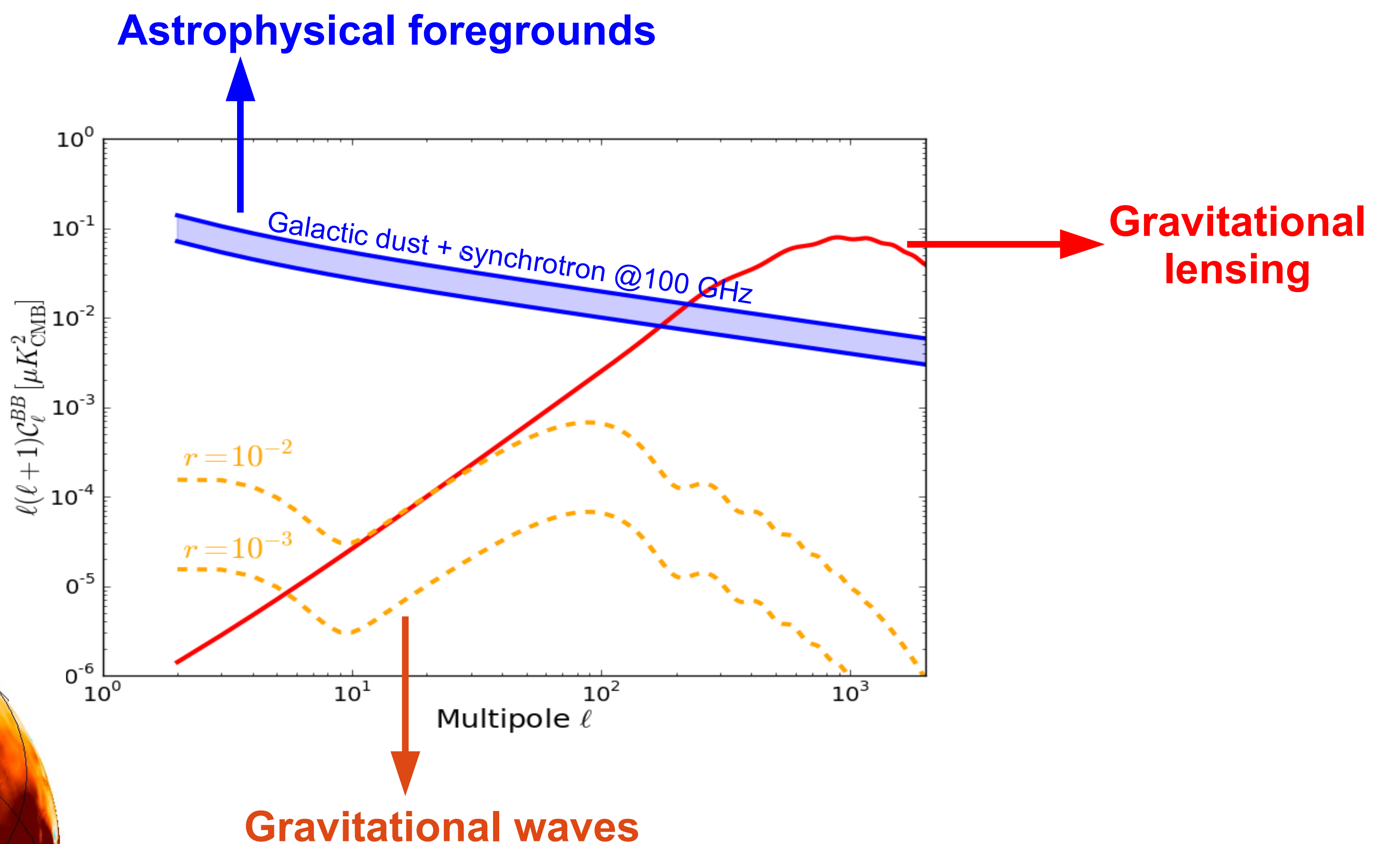

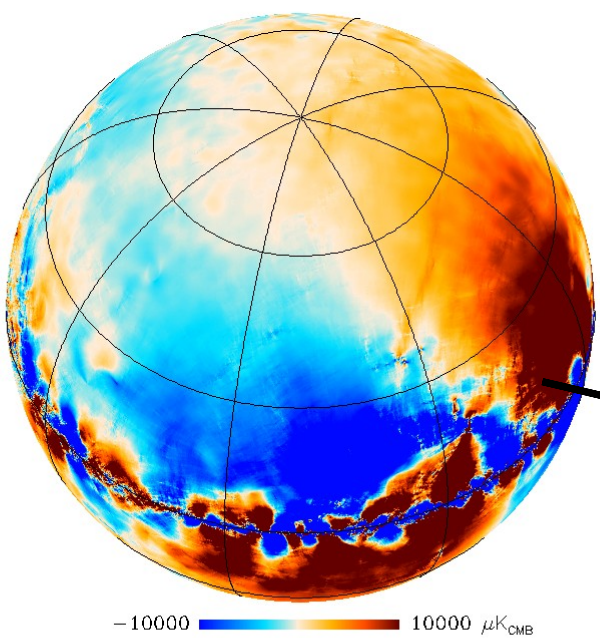

This is the B-mode signal we see in the sky: our Galaxy!

Short digression

Anisotropic μ-type distortions at $z > 10^4$

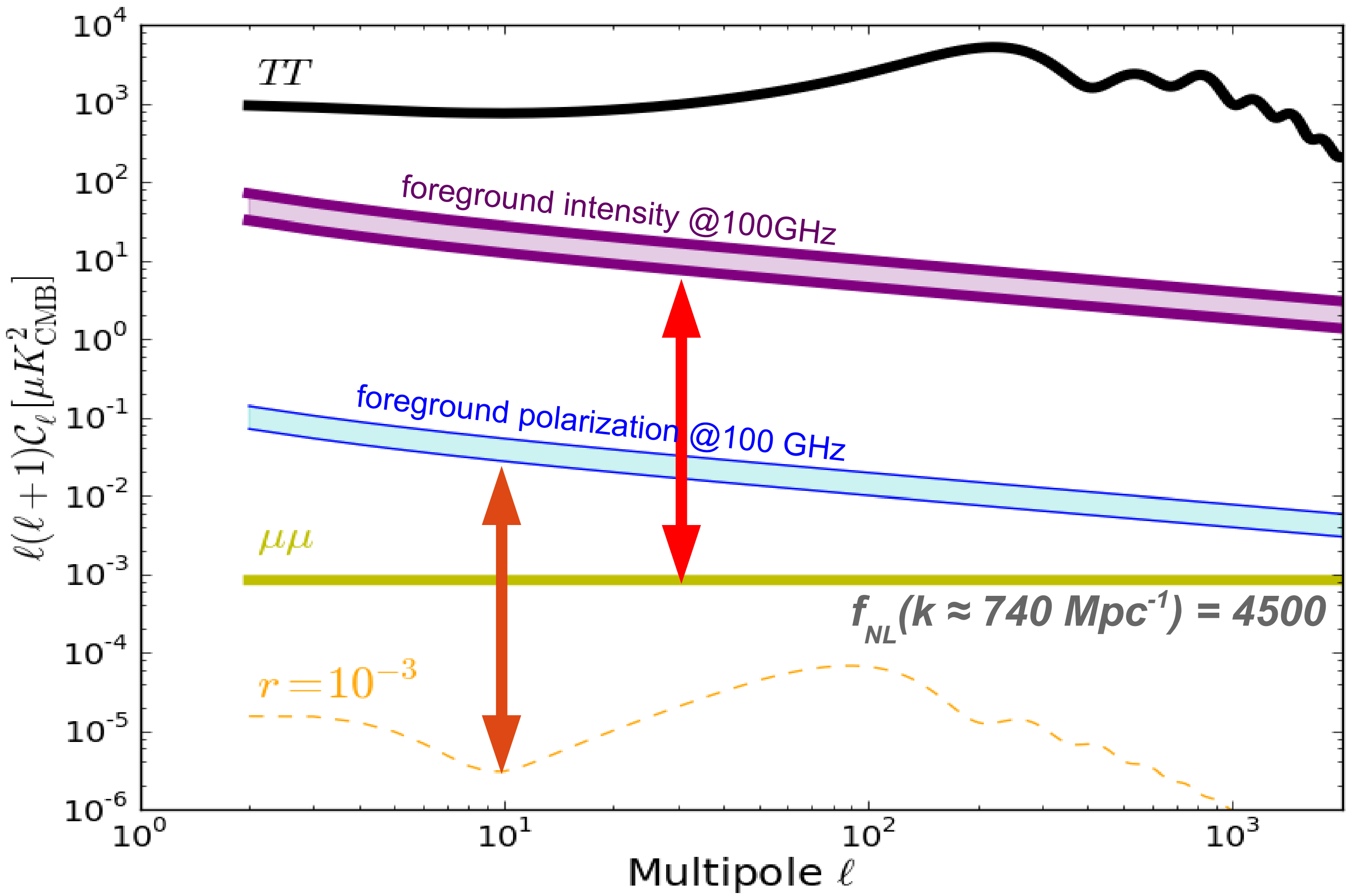

- ***Same dynamic range than for primordial B-modes at $r \sim 10^{-3}$***

  → to be definitely considered by future CMB satellites!

- ***Anisotropic μ-type distortions (Pajer & Zaldarriaga 2012) caused by exciting physics at pre-recombination epochs:***

  → Silk damping, annihilation/decay of DM particles, primordial BH, ...

Anisotropic μ-type distortions at $z > 10^4$

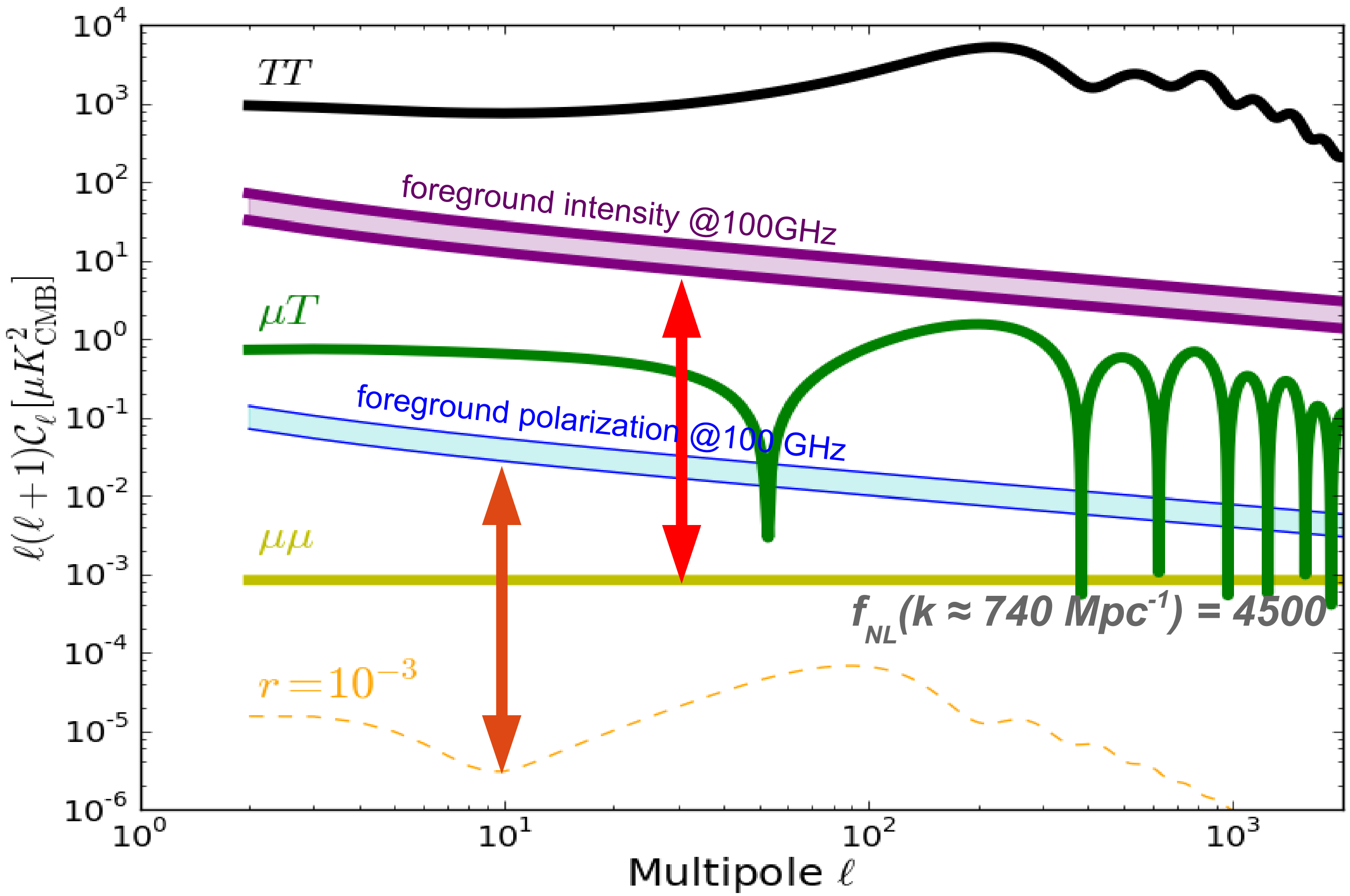

μ-T correlation signal between CMB temperature and μ-distortion anisotropies

→ ***even more accessible signal, allowing to constrain $f_{NL}(k \approx 740\ Mpc^{-1})$***

→ ***to be definitely considered by future CMB satellites!***

More details in Remazeilles & Chluba (2018): arXiv:1802.10101

CMB B-mode vs Foregrounds

Remazeilles et al (2017), for the CORE collaboration

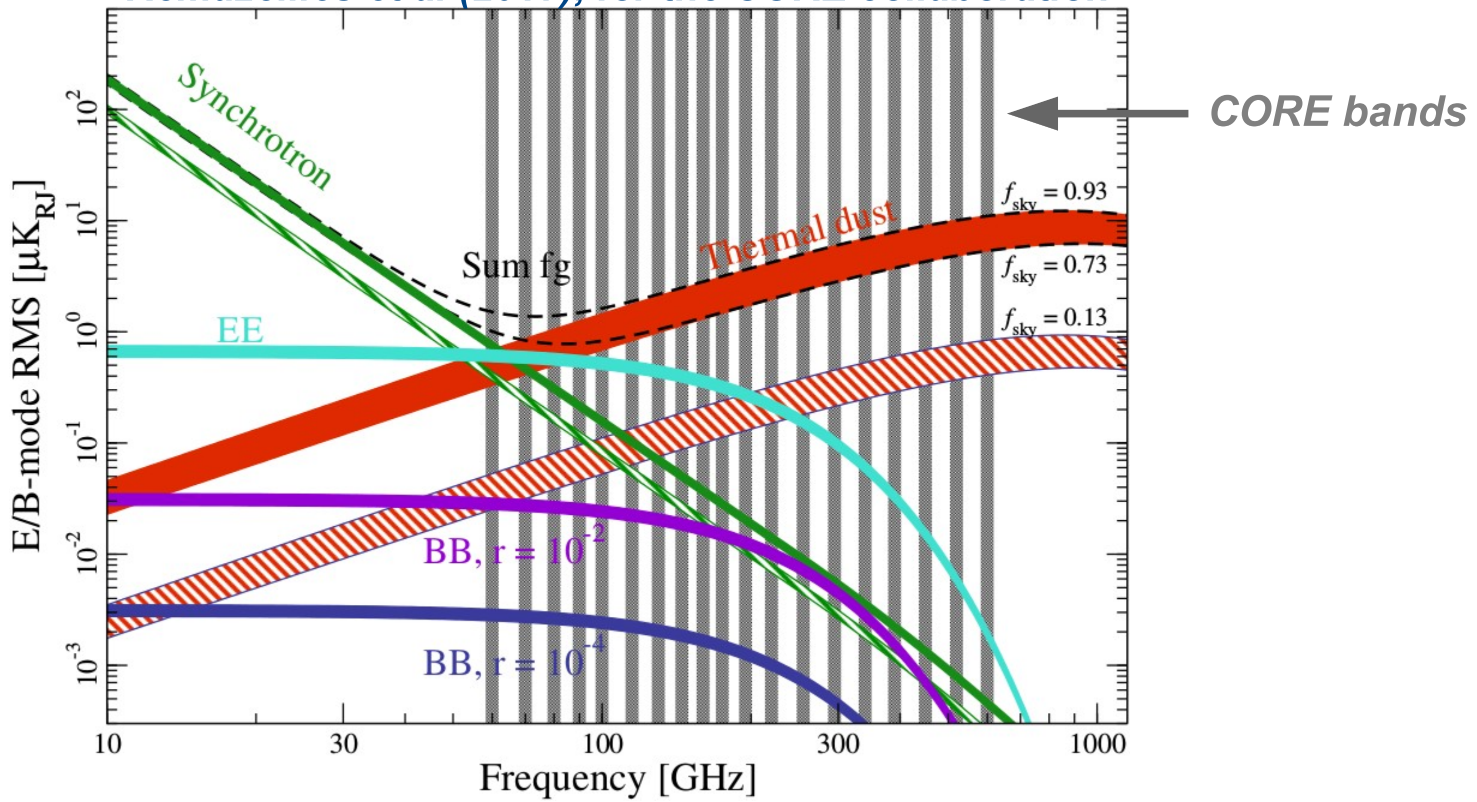

- **Polarization <u>less complex</u> than intensity (fewer foregrounds) but <u>more challenging</u> (weaker signal):**

  → *Very large dynamic range between CMB B-mode and foregrounds*

  → *Component separation much more sensitive to foreground uncertainties!*

- **Foregrounds cannot be avoided by limiting the frequency range of observations**

  → *At ~300 GHz, synchrotron and CMB B-modes ($r=10^{-2}$) have similar amplitude and colour!*

  → *A broad frequency coverage is essential to break those spectral degeneracies*

Future CMB satellites aim at detecting $r = 10^{-3}$

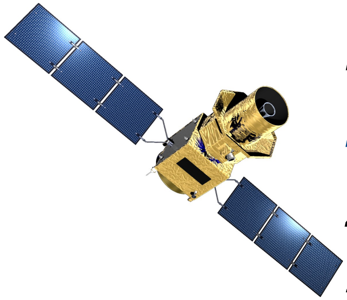

LiteBIRD (JAXA – Phase A)

Matsumura et al, 2013

40 – 402 GHz

2.5 μK.arcmin

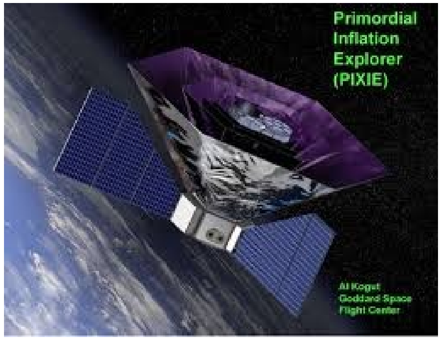

PIXIE (NASA?)

Kogut et al., 2011

30 – 6000 GHz

6.6 μK.arcmin
for Δν=30 GHz

CORE (ESA? ISRO?)

Delabrouille et al, 2018

60 – 600 GHz

1.7 μK.arcmin

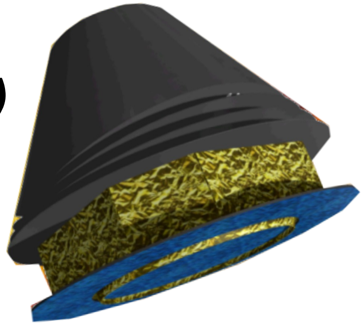

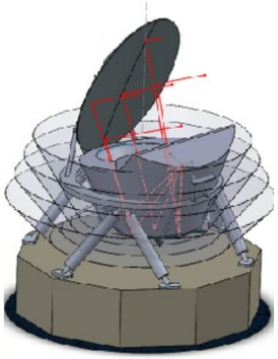

PICO (NASA?)

S. Hannany, priv. comm.

21 – 800 GHz

1 μK.arcmin

Why going into space?

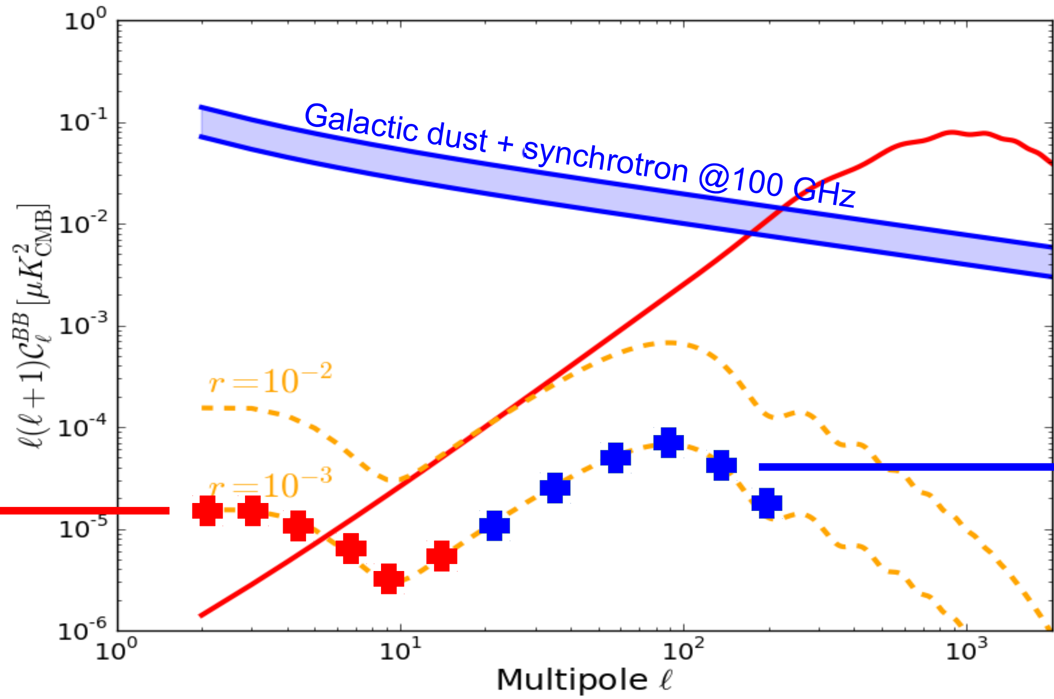

Large scales measurable from space only

Small scales measurable from ground and space

Why going into space?

Large scales measurable from space only

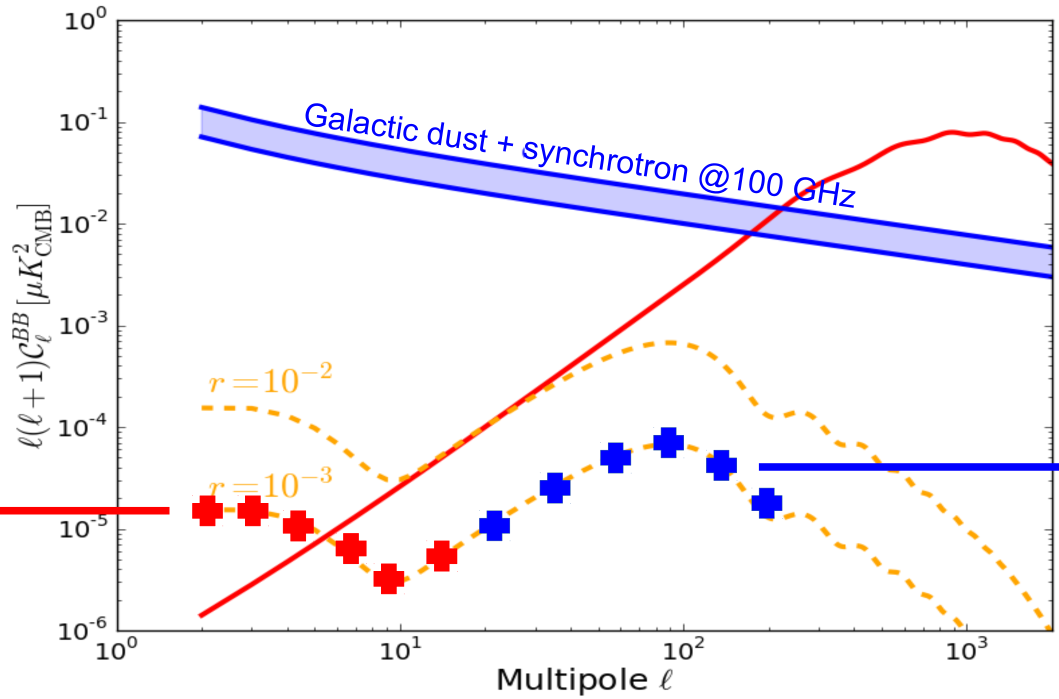

Small scales measurable from ground and space

- ***Problem*: at recombination scales (20 < ℓ < 200), measurements may be fooled by many kind of power spectra degeneracies between primordial B-modes, lensing B-modes, extragalactic sources, and noise (similar slopes)**

Why going into space?

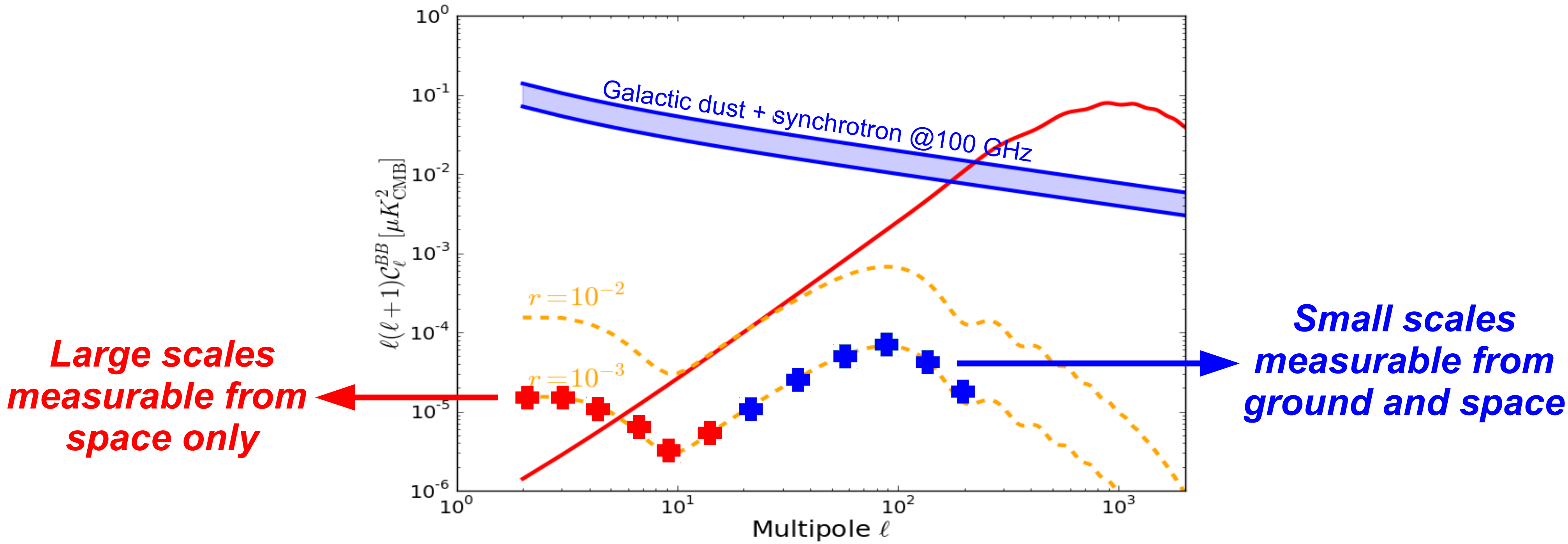

- ***Problem*: at recombination scales (20 < ℓ < 200), measurements may be fooled by many kind of power spectra degeneracies between primordial B-modes, lensing B-modes, extragalactic sources, and noise (similar slopes)**
- ***Detecting the reionization peak (2 < ℓ < 20) from space* will allow to break power spectrum degeneracies, providing better evidence for primordial B-mode detection**

CORE

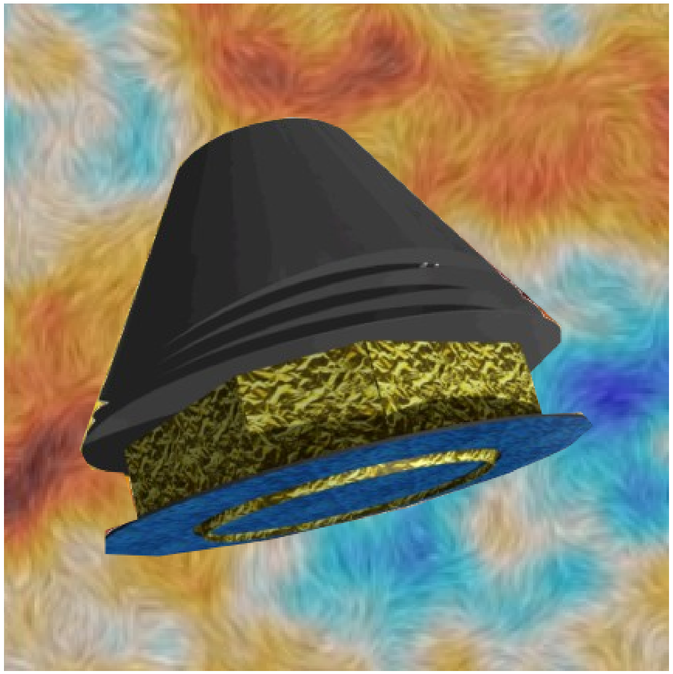

→ ***Not selected by ESA, but we have cleared the path on the foreground challenges***

→ ***Series of 10 CORE papers (JCAP special issue)***

Exploring Cosmic Origins with CORE: B-mode Component Separation

M. Remazeilles,[1] A. J. Banday,[2,3] C. Baccigalupi,[4,5] S. Basak,[6,4] A. Bonaldi,[1] G. De Zotti,[7] J. Delabrouille,[8] C. Dickinson,[1] H. K. Eriksen,[9] J. Errard,[10] R. Fernandez-Cobos,[11] U. Fuskeland,[9] C. Hervías-Caimapo,[1] M. López-Caniego,[12] E. Martinez-González,[11] M. Roman,[13] P. Vielva,[11] I. Wehus,[9] A. Achucarro,[14,15] P. Ade,[16] R. Allison,[17] M. Ashdown,[18,19] M. Ballardini,[20,21,22] R. Banerji,[8] N. Bartolo,[23,24,7] J. Bartlett,[8] D. Baumann,[25] M. Bersanelli,[26,27] M. Bonato,[28,4] J. Borrill,[29] F. Bouchet,[30] F. Boulanger,[31] T. Brinckmann,[32] M. Bucher,[8] C. Burigana,[21,33,22] A. Buzzelli,[34,35,36] Z.-Y. Cai,[37] M. Calvo,[38] C.-S. Carvalho,[39] G. Castellano,[40] A. Challinor,[25] J. Chluba,[1] S. Clesse,[32] I. Colantoni,[40] A. Coppolecchia,[34,41] M. Crook,[42] G. D'Alessandro,[34,41] P. de Bernardis,[34,41] G. de Gasperis,[34,36] J.-M. Diego,[11] E. Di Valentino,[30,43] S. Feeney,[18,44] S. Ferraro,[45] F. Finelli,[21,22] F. Forastieri,[46] S. Galli,[30] R. Genova-Santos,[47,48] M. Gerbino,[49,50] J. González-Nuevo,[51] S. Grandis,[52,53] J. Greenslade,[18] S. Hagstotz,[52,53] S. Hanany,[54] W. Handley,[18,19] C. Hernandez-Monteagudo,[55] M. Hills,[42] E. Hivon,[30] K. Kiiveri,[56,57] T. Kisner,[29] T. Kitching,[58] M. Kunz,[59] H. Kurki-Suonio,[56,57] L. Lamagna,[34,41] A. Lasenby,[18,19] M. Lattanzi,[46] J. Lesgourgues,[32] A. Lewis,[60] M. Liguori,[23,24,7] V. Lindholm,[56,57] G. Luzzi,[34] B. Maffei,[31] C.J.A.P. Martins,[61] S. Masi,[34,41] D. McCarthy,[62] J.-B. Melin,[63] A. Melchiorri,[34,41] D. Molinari,[33,46,21] A. Monfardini,[38] P. Natoli,[33,46] M. Negrello,[16] A. Notari,[64] A. Paiella,[34,41] D. Paoletti,[21] G. Patanchon,[8] M. Piat,[8] G. Pisano,[16] L. Polastri,[33,45] G. Polenta,[65,66] A. Pollo,[67] V. Poulin,[32,68] M. Quartin,[69,70] J.-A. Rubino-Martin,[47,48] L. Salvati,[34,41] A. Tartari,[8] M. Tomasi,[26] D. Tramonte,[47] N. Trappe,[62] T. Trombetti,[21,33,22] C. Tucker,[16] J. Valiviita,[56,57] R. Van de Weijgaert,[71,72] B. van Tent,[73] V. Vennin,[74] N. Vittorio,[35,36] K. Young,[54] and M. Zannoni,[75,76] for the CORE collaboration.

Accepted by JCAP (2017)

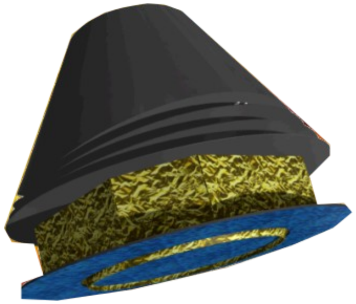

CORE specifications

Frequency [GHz]	Beam [arcmin]	Q and U noise RMS [μK.arcmin]
60	17.87	10.6
70	15.39	10.0
80	13.52	9.6
90	12.08	7.3
100	10.92	7.1
115	9.56	7.0
130	8.51	5.5
145	7.68	5.1
160	7.01	5.2
175	6.45	5.1
195	5.84	4.9
220	5.23	5.4
255	4.57	7.9
295	3.99	10.5
340	3.49 (4.0)	15.7
390	3.06 (4.0)	31.1
450	2.65 (4.0)	64.9
520	2.29 (4.0)	164.8
600	1.98 (4.0)	506.7

- **100% of the sky**
- **19 frequency bands: 60 – 600 GHz**
- **Aggregated sensitivity: 1.7 μK.arcmin**
- **High spatial resolution allowing for 60% delensing**

  Challinor et al 2017, for the CORE collaboration

Delabrouille et al 2017, for the CORE collaboration

CORE sky simulations: Stokes Q maps

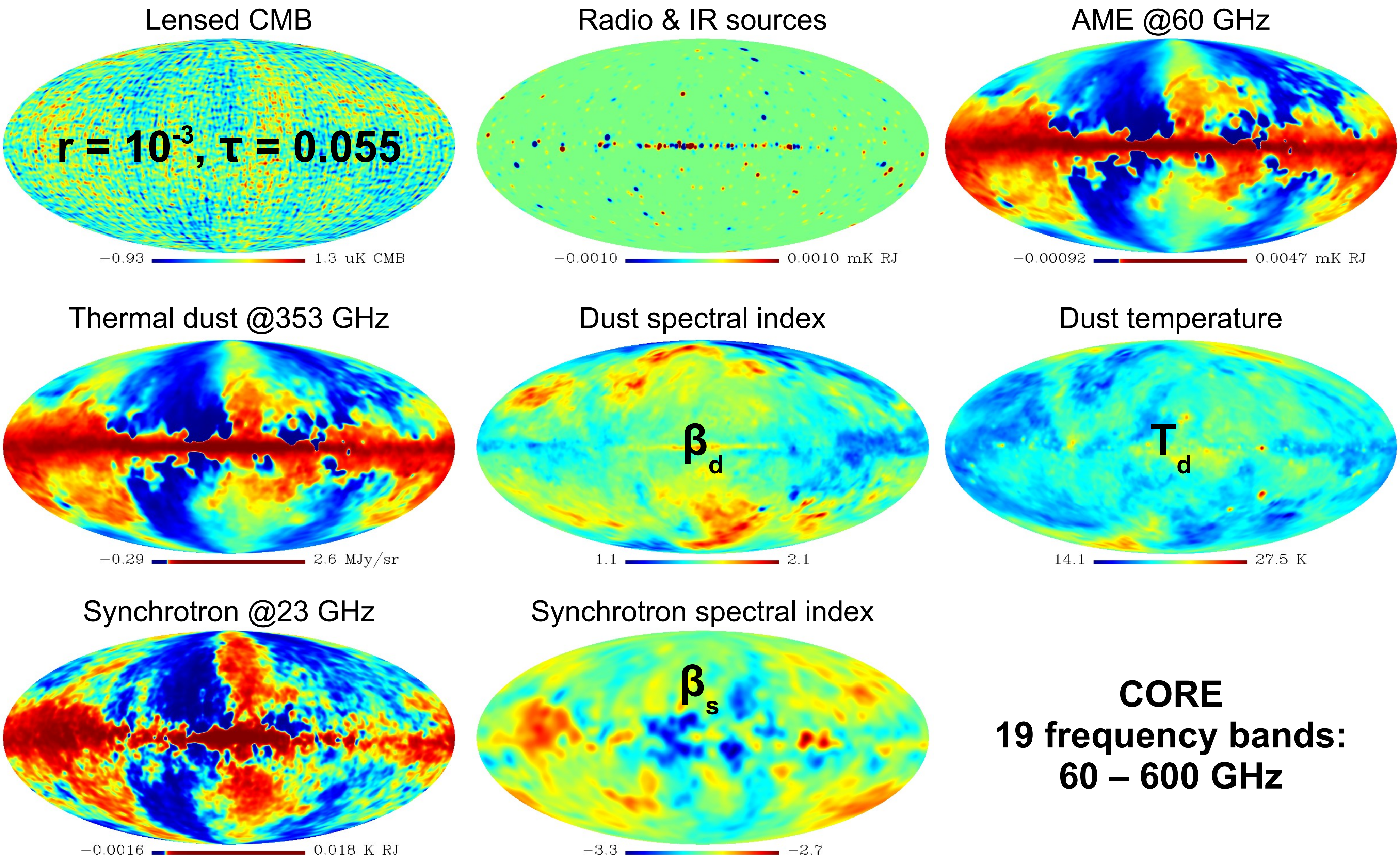

CORE
19 frequency bands:
60 – 600 GHz

smoothed to 1°
for illustration purposes

Remazeilles et al 2017, for the CORE collaboration

Component separation methods

- **COMMANDER** – *Eriksen et al 2004, 2008 ; Remazeilles et al 2016, 2017*

  Bayesian multi-component spectral fit in each pixel through Gibbs sampling

- **SMICA** – *Delabrouille et al 2003 ; Cardoso et al 2008*

  Blind power spectra fit in harmonic space

- **NILC** – *Delabrouille et al 2009 ; Remazeilles et al 2011 ; Basak et al 2012, 2013*

  Minimum-variance internal linear combination in wavelet space

- **X-FORECAST** – *Errard et al 2016 ; Stompor et al 2016*

  Spectral fit of foreground mixing matrix + linear combination

---

The first 3 algorithms have been thoroughly used on Planck data
Planck 2015 results. IX., A&A 2016

The 4 algorithms have been employed on CORE simulations for B-mode detection forecasts
Remazeilles et al, for the CORE collaboration, JCAP 2017

CORE reconstruction of the primordial B-mode
– without lensing –

$r = 10^{-2}$

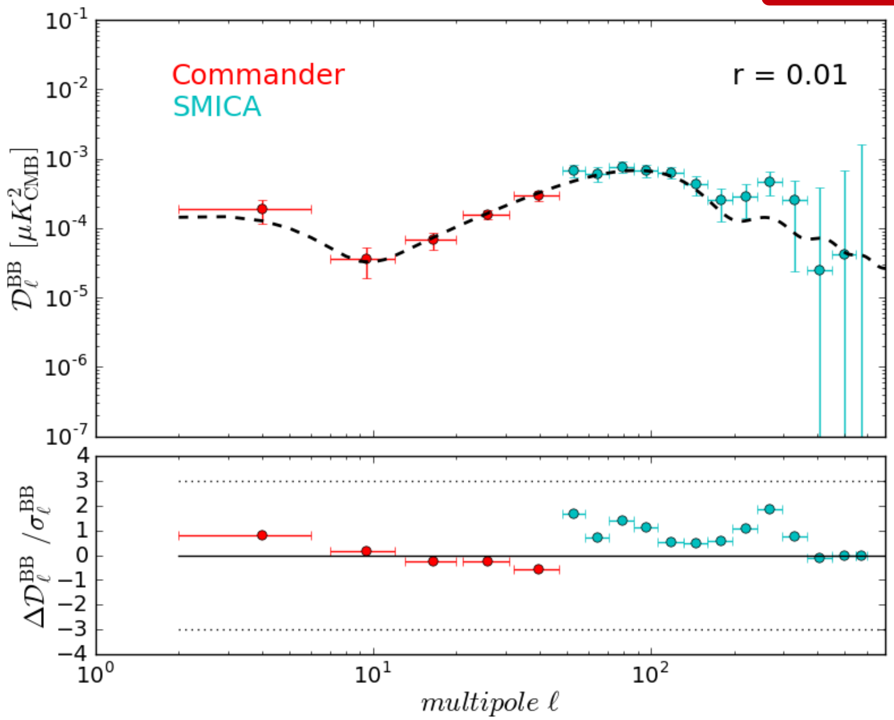

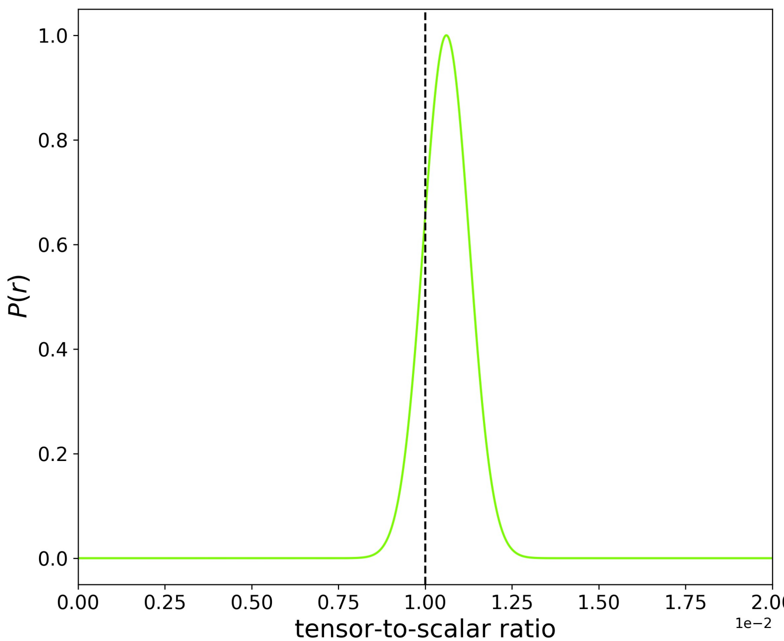

14σ detection of $r = 10^{-2}$ after foreground cleaning

Remazeilles et al 2017, for the CORE collaboration

CORE reconstruction of the primordial B-mode
– without lensing –

r = 5 × 10^{-3}

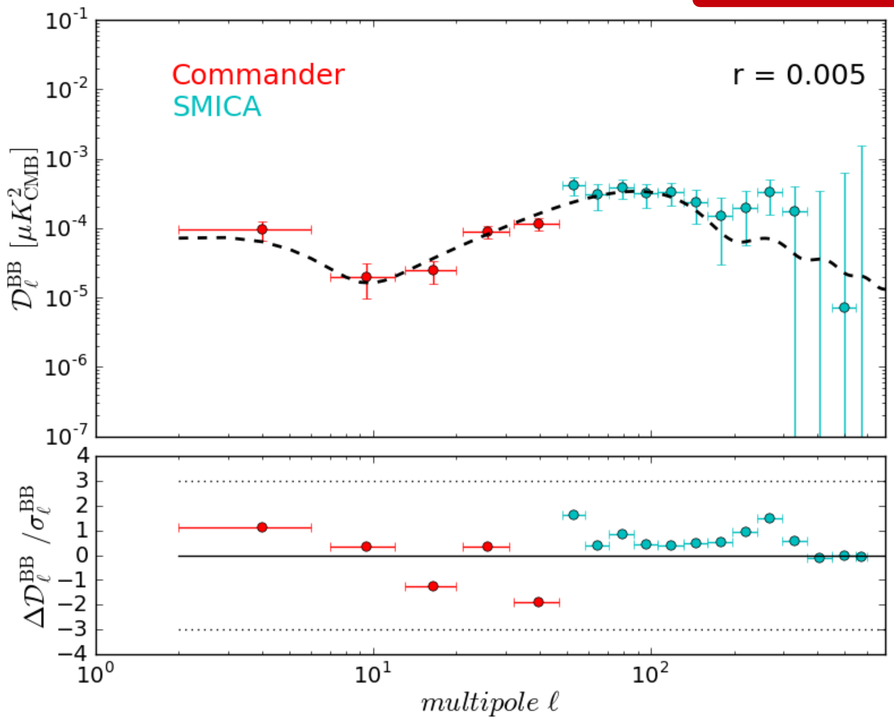

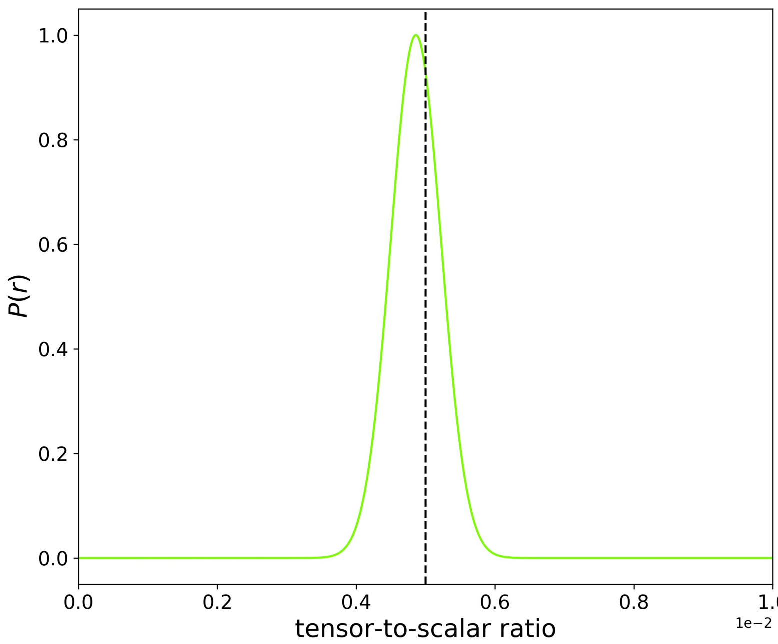

12σ detection of r = 5 × 10^{-3} after foreground cleaning

Remazeilles et al 2017, for the CORE collaboration

CORE reconstruction of the primordial B-mode

– with lensing –

$r = 5 \times 10^{-3}$

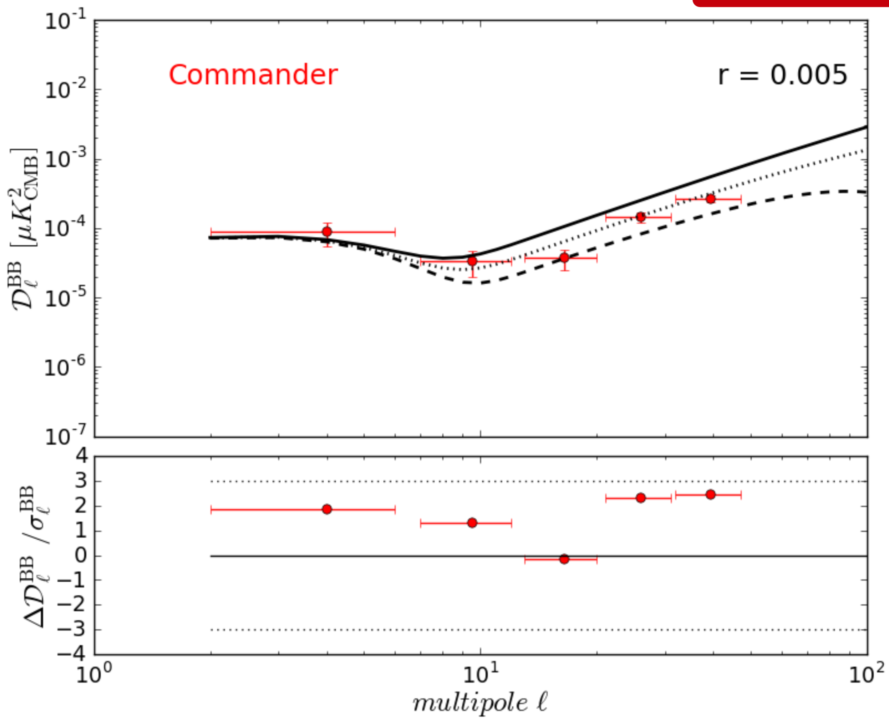

r = (5.4 ± 1.5) × 10^{-3}

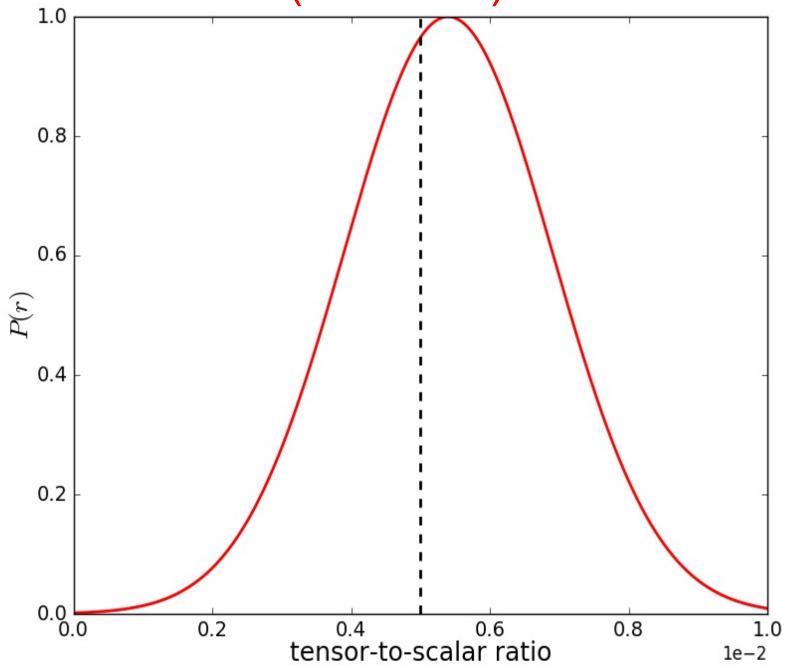

4σ detection of $r = 5 \times 10^{-3}$
after foreground cleaning and 60% delensing

Remazeilles et al 2017, for the CORE collaboration

CORE reconstruction of the primordial B-mode
– without lensing –

$r = 10^{-3}$

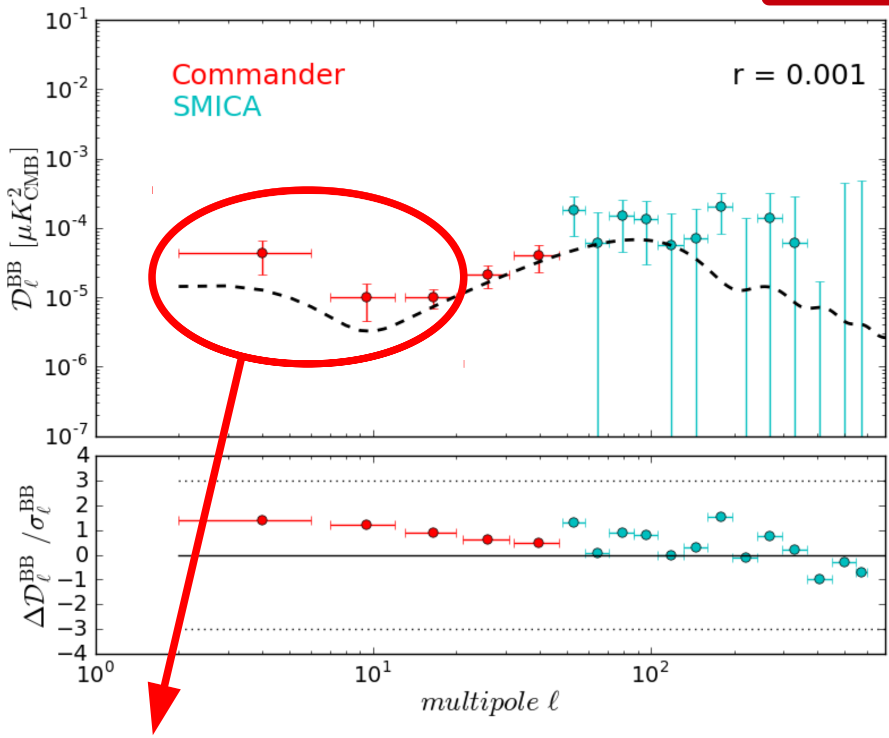

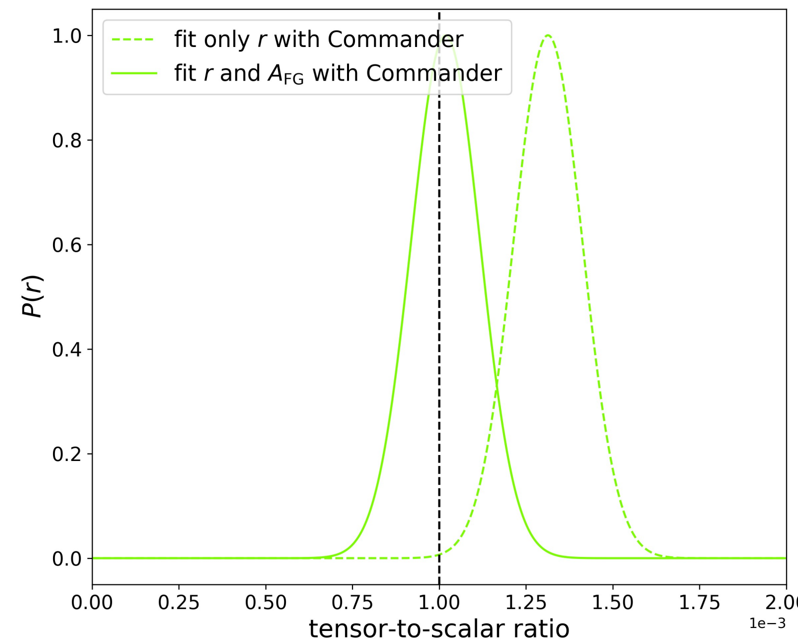

foreground residuals!

3σ bias on $r = 10^{-3}$ after foreground cleaning

Remazeilles et al 2017, for the CORE collaboration

Lack of frequencies < 60 GHz

Error $\Delta\beta_{synch}$ ~ 2% $\Rightarrow$ error Δr ~ 10^{-3} when extrapolated from 23 to 145 GHz

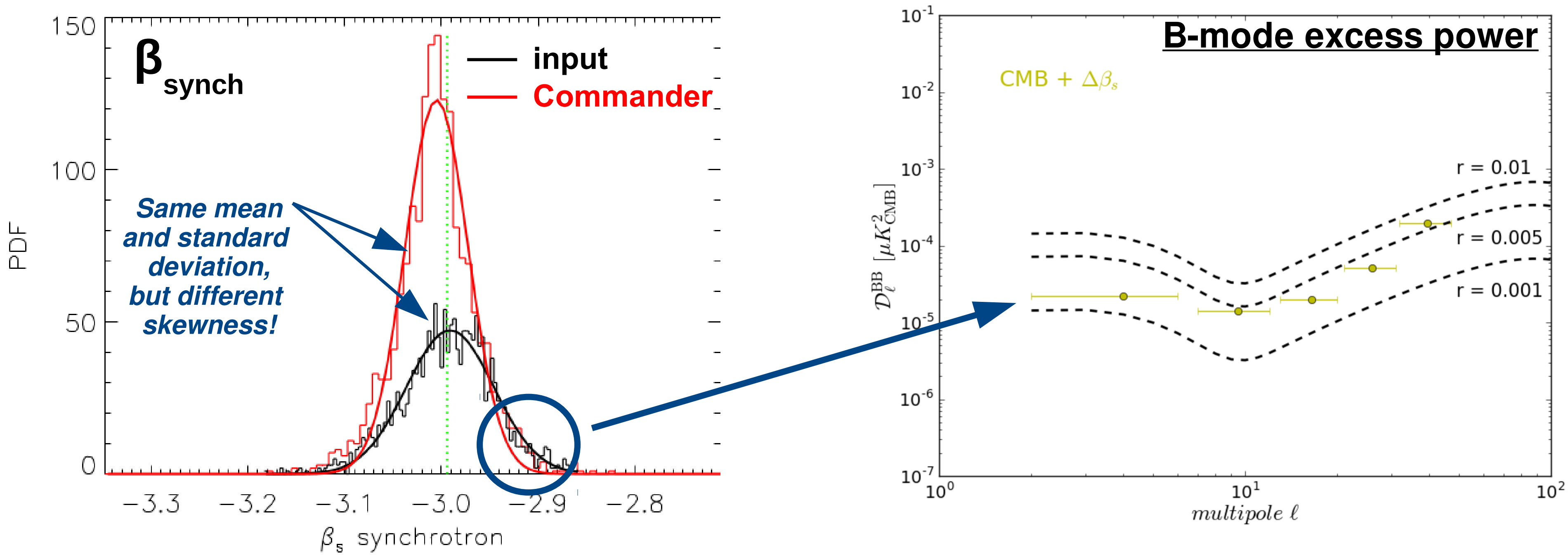

Remazeilles et al 2017, for the CORE collaboration

Sub-percent precision on foreground spectral parameters is required to allow the detection of B-modes at the level of $r = 10^{-3}$

On the importance
of a broad frequency range

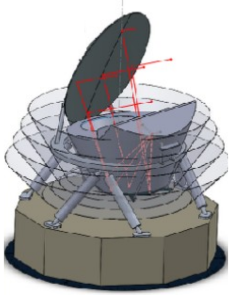

PICO

- **21 frequency bands : 21 – 800 GHz**
- **Overall sensitivity : ~ 1 µK.arcmin**

CMBP						
del nu/nu	0,25		del center	1,2		
nu1	30	GHz				
	nu	**nu_low**	**nu_high**	**del nu**	**FWHM**	**PolWeight**
Band#	**(GHz)**	**(GHz)**	**(GHz)**	**(GHz)**	**(arcmin)**	**(uk*arcmin)**
1	21	18,2	23,4	5,2	40,9	50
2	25	21,9	28,1	6,3	34,1	33
3	30	26,3	33,8	7,5	28,4	22,4
4	36,0	31,5	40,5	9,0	23,7	15
5	43,2	37,8	48,6	10,8	19,7	9,1
6	51,8	45,4	58,3	13,0	16,4	7
7	62,2	54,4	70,0	15,6	13,7	5
8	74,6	65,3	84,0	18,7	11,4	4
9	89,6	78,4	100,8	22,4	9,5	3,2
10	107,5	94,1	120,9	26,9	7,9	2,9
11	129,0	112,9	145,1	32,2	6,6	2,7
12	154,8	135,4	174,1	38,7	5,5	2,6
13	185,8	162,5	209,0	46,4	4,6	3,6
14	222,9	195,0	250,8	55,7	3,8	5,3
15	267,5	234,0	300,9	66,9	3,2	9
16	321,0	280,9	361,1	80,2	2,7	16,0
17	385,2	337,0	433,3	96,3	2,2	32
18	462,2	404,4	520,0	115,6	1,8	75
19	554,7	485,3	624,0	138,7	1,5	220,0
20	665,6	582,4	748,8	166,4	1,3	1100
21	798,7	698,9	898,5	199,7	1,1	10000,0

PICO reconstruction of primordial B-modes

21 – 800 GHz

$r = 10^{-3}$

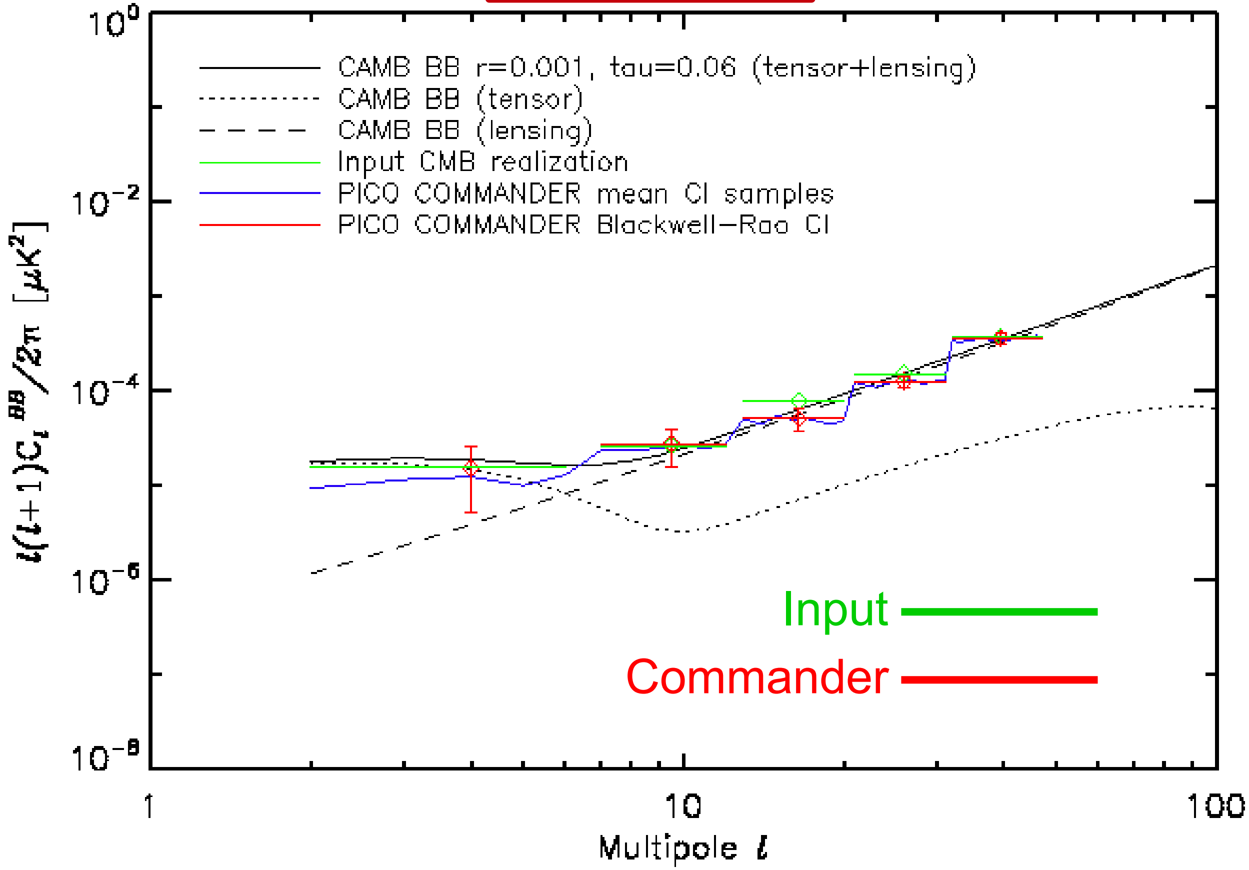

Foregrounds:

- *Synchrotron (power-law with curvature)*
- *Thermal dust (MBB)*

$\sigma(r = 10^{-3}) = 0.4 \times 10^{-3}$

after foreground cleaning

M. Remazeilles

PICO reconstruction of primordial B-modes
43 – 462 GHz

r = 10^{-3}

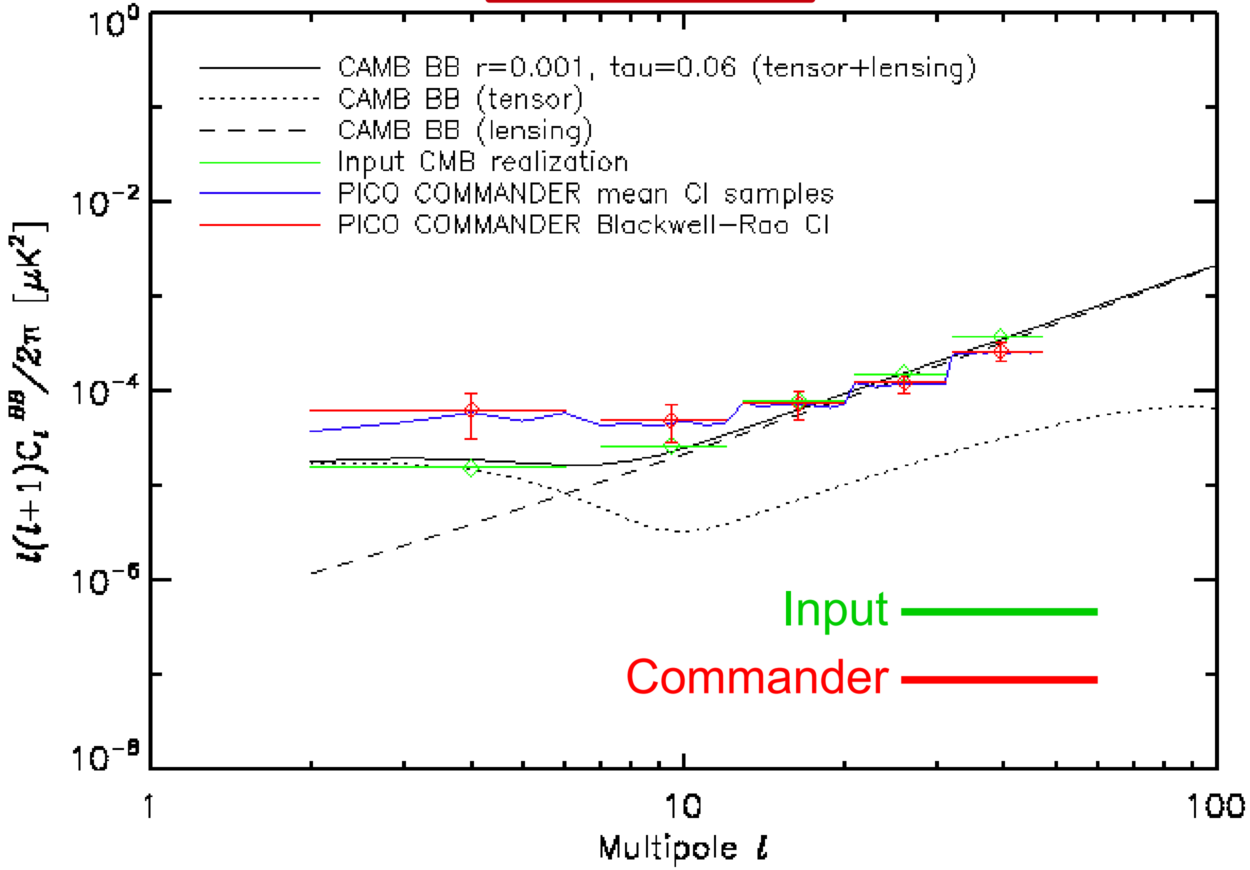

Foregrounds:

- *Synchrotron (power-law with curvature)*
- *Thermal dust (MBB)*

Narrowing the frequency range of observations causes biases on large-scales due to foregrounds

M. Remazeilles

COMMANDER results on foregrounds
PICO **21 – 800 GHz**

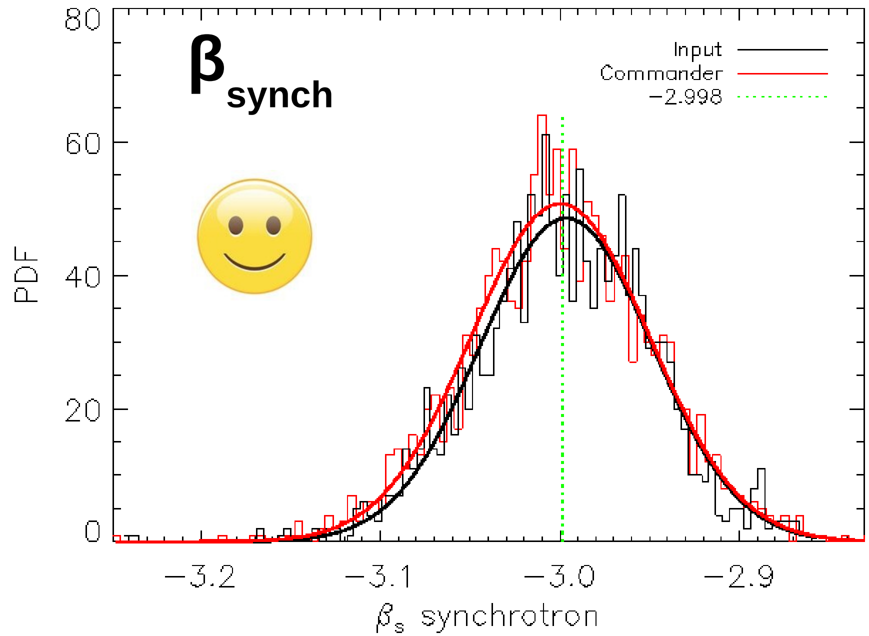

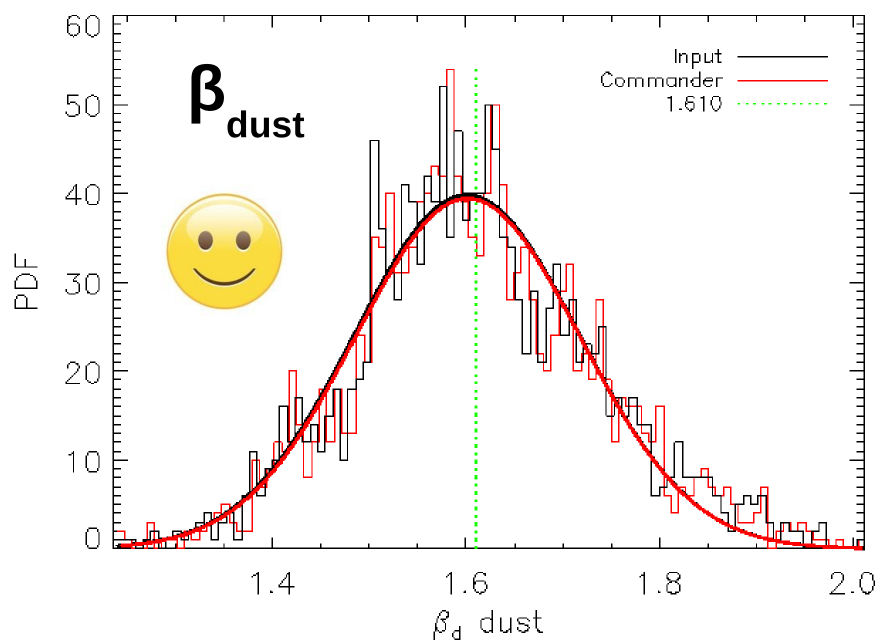

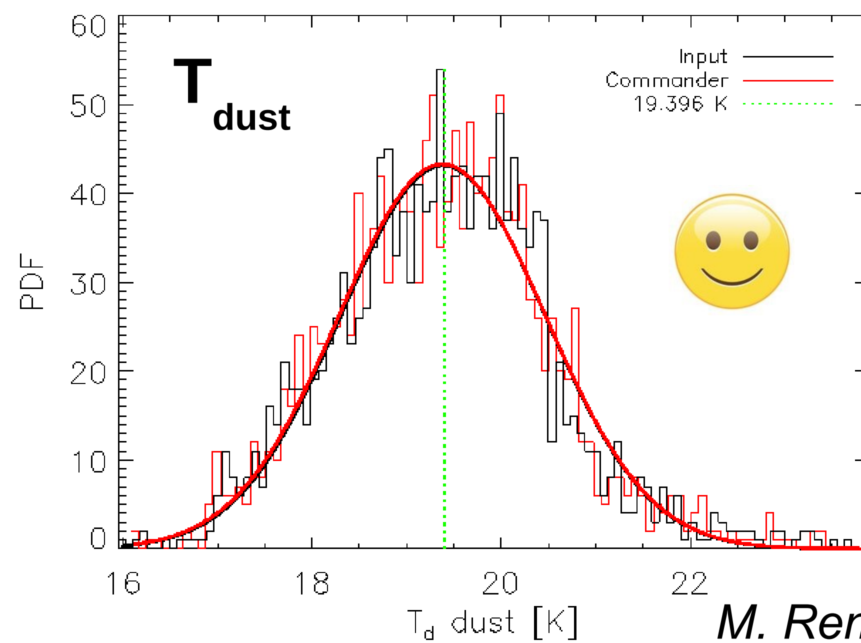

M. Remazeilles

COMMANDER results on foregrounds
PICO **43 – 462 GHz**

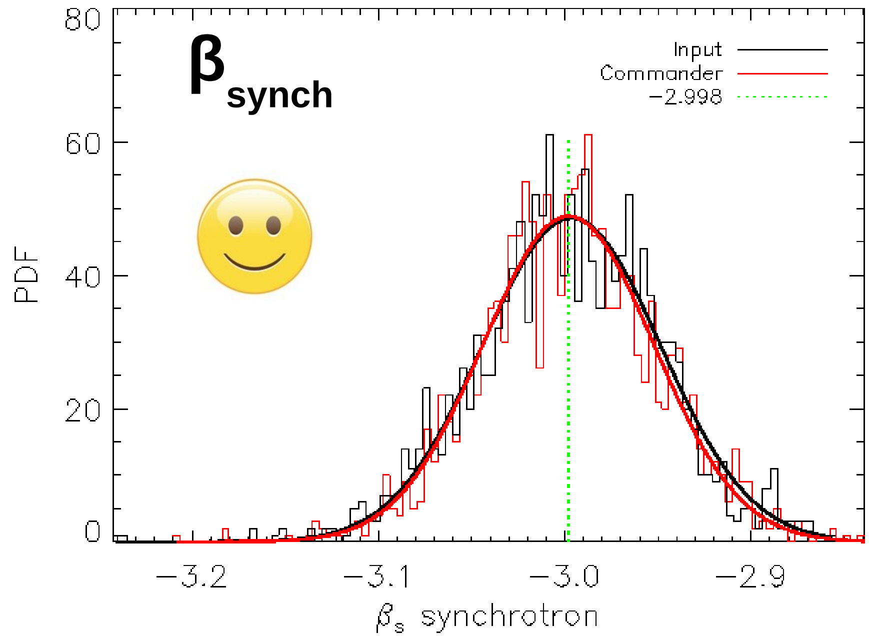

Lack of frequency range / high frequencies

↓

Lack of precision/constraint on T_{dust}

↓

Translates into a bias on CMB B-mode by extrapolation towards CMB frequencies

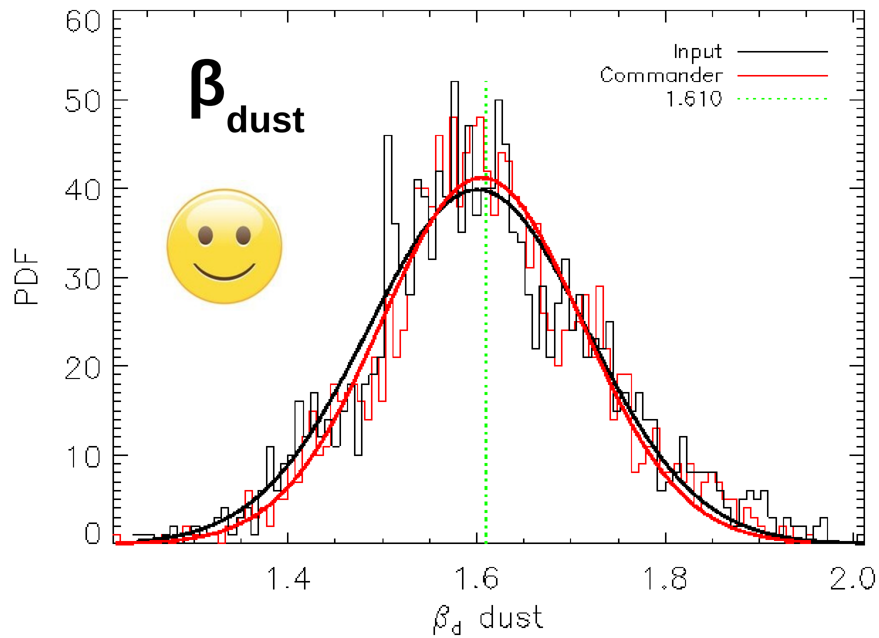

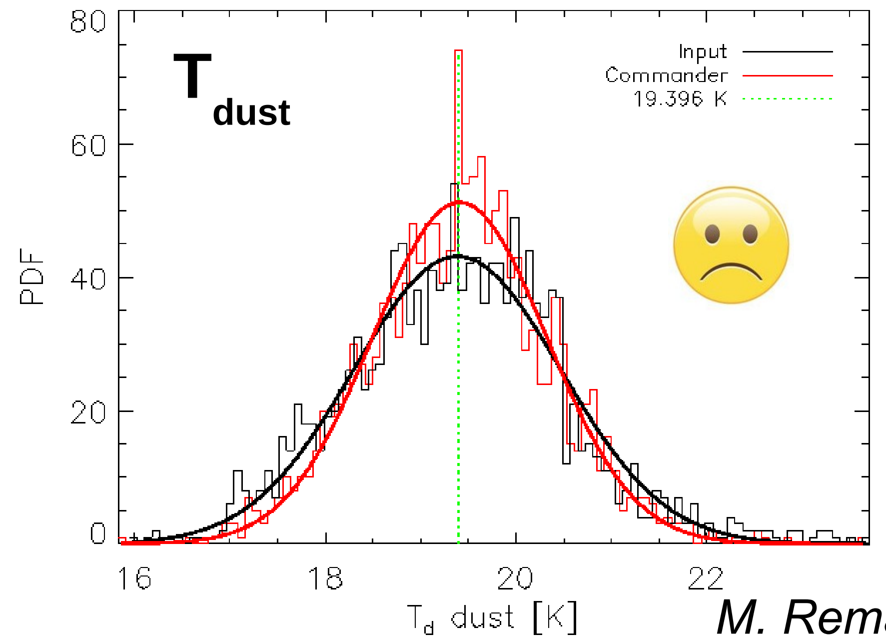

M. Remazeilles

PICO
21 – 800 GHz

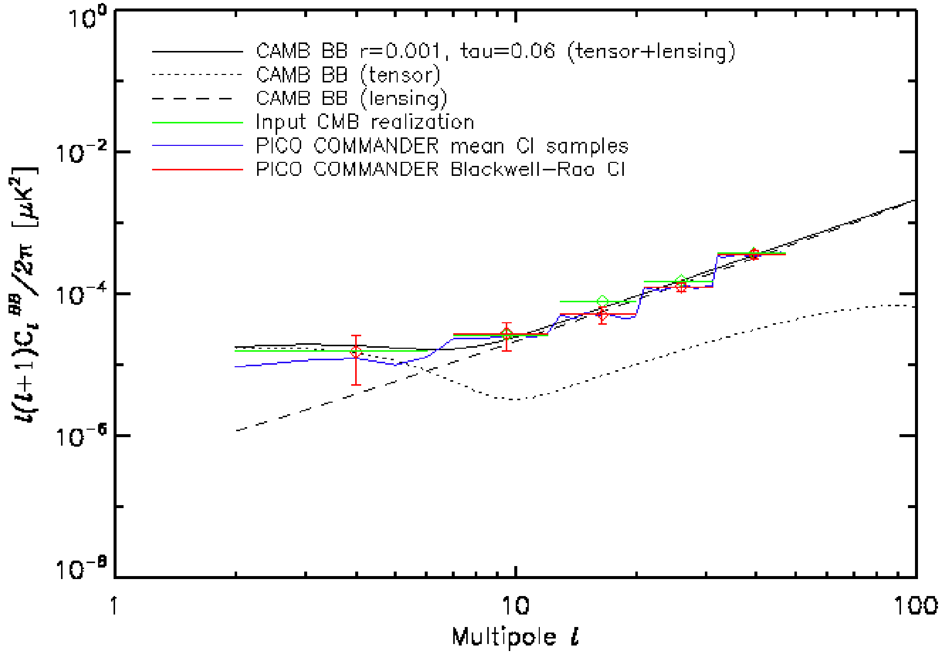

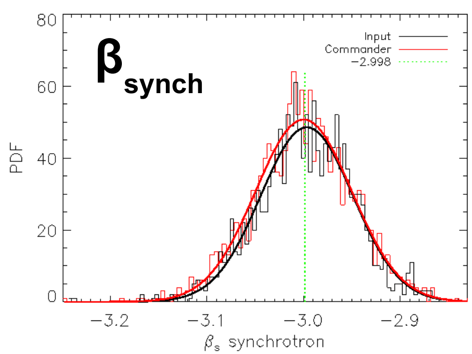

σ(r=10^-3) = 0.4 × 10^-3

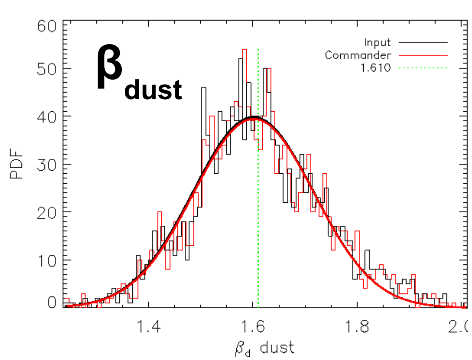

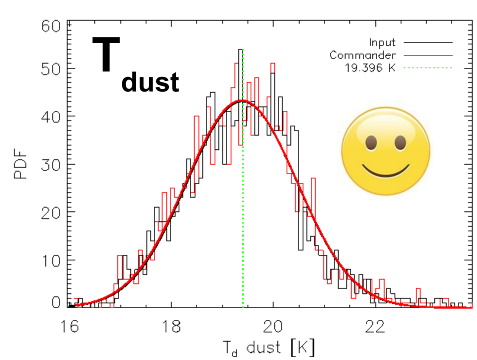

PICO
43 – 462 GHz

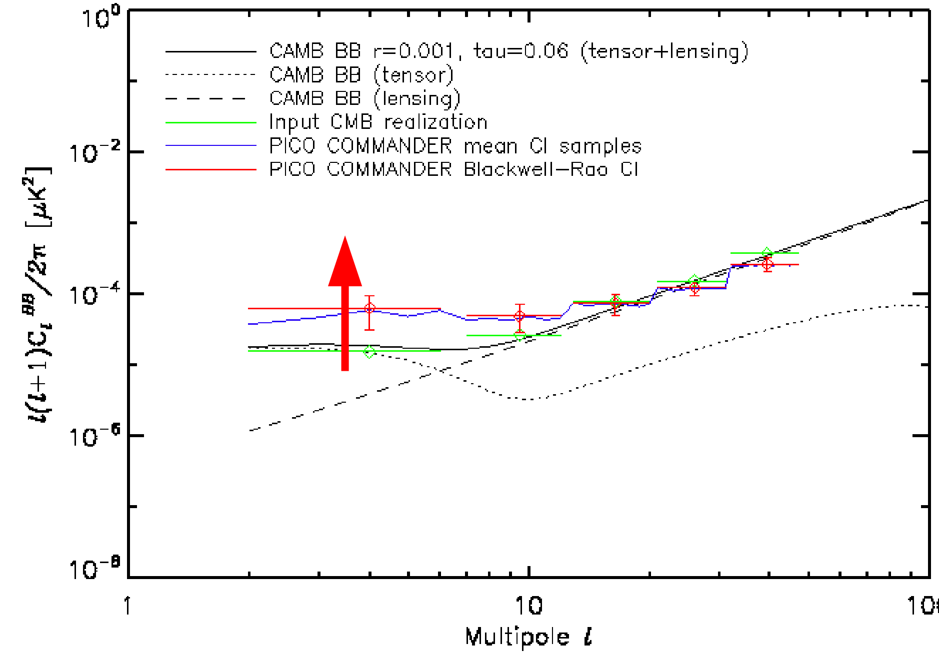

σ(r=10^-3) = 0.7 × 10^-3

(75% increase)

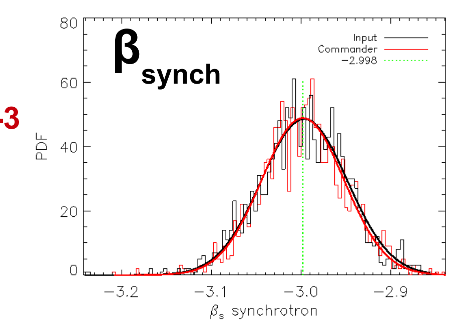

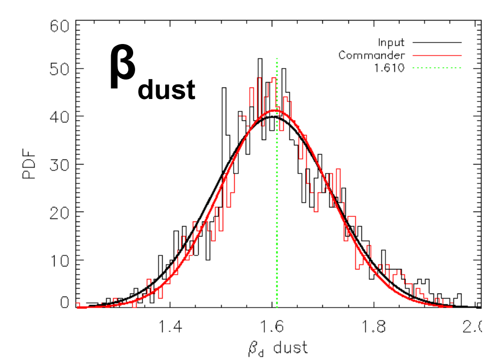

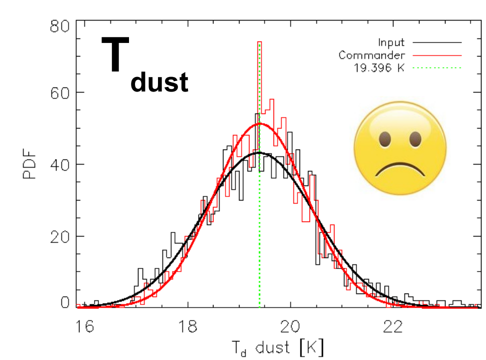

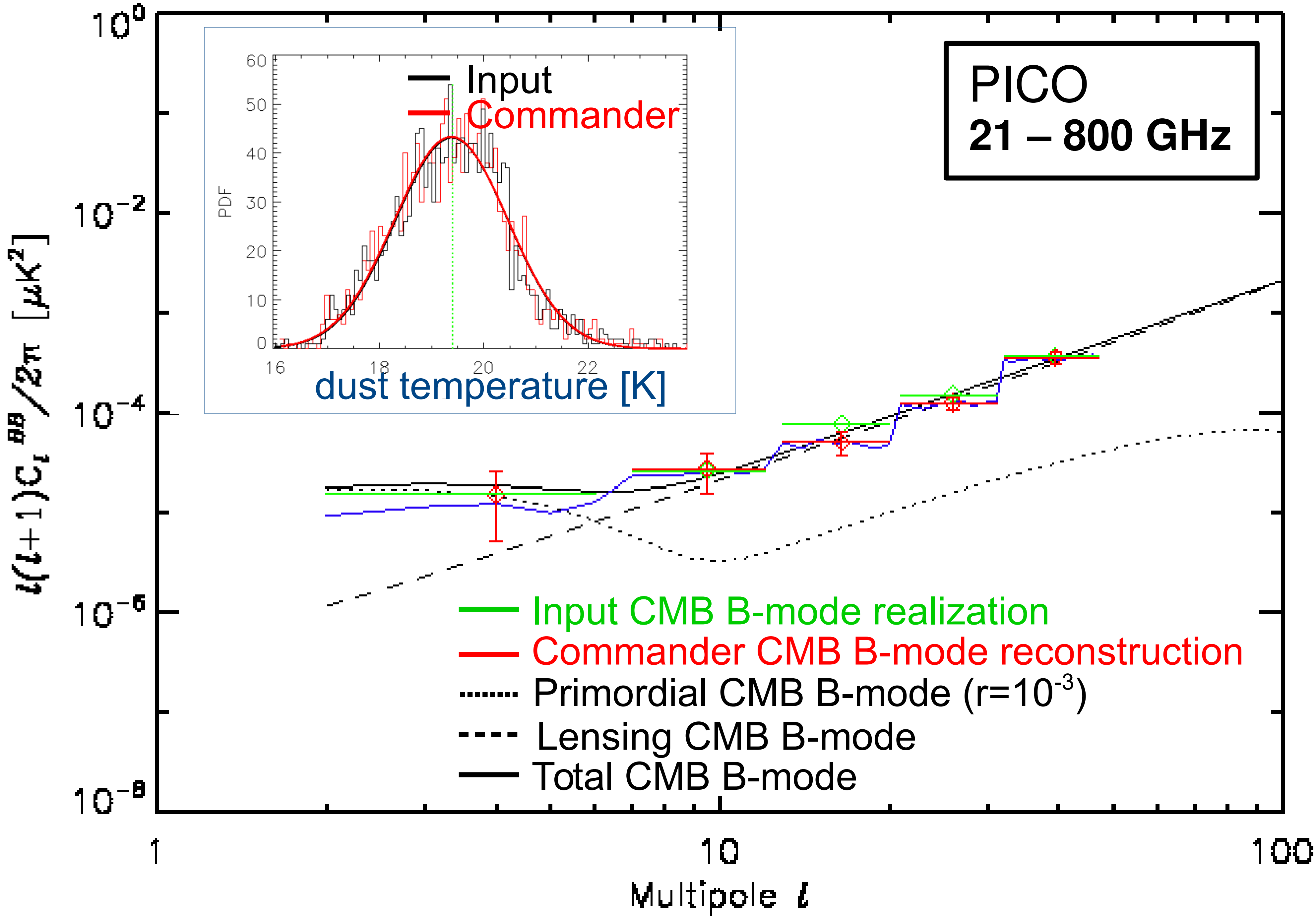

PICO
21 – 800 GHz
Input
Commander
PDF
dust temperature [K]
Input CMB B-mode realization
Commander CMB B-mode reconstruction
Primordial CMB B-mode (r=10^-3)
Lensing CMB B-mode
Total CMB B-mode
Multipole ℓ
ℓ(ℓ+1)C_ℓ^BB/2π [μK^2]

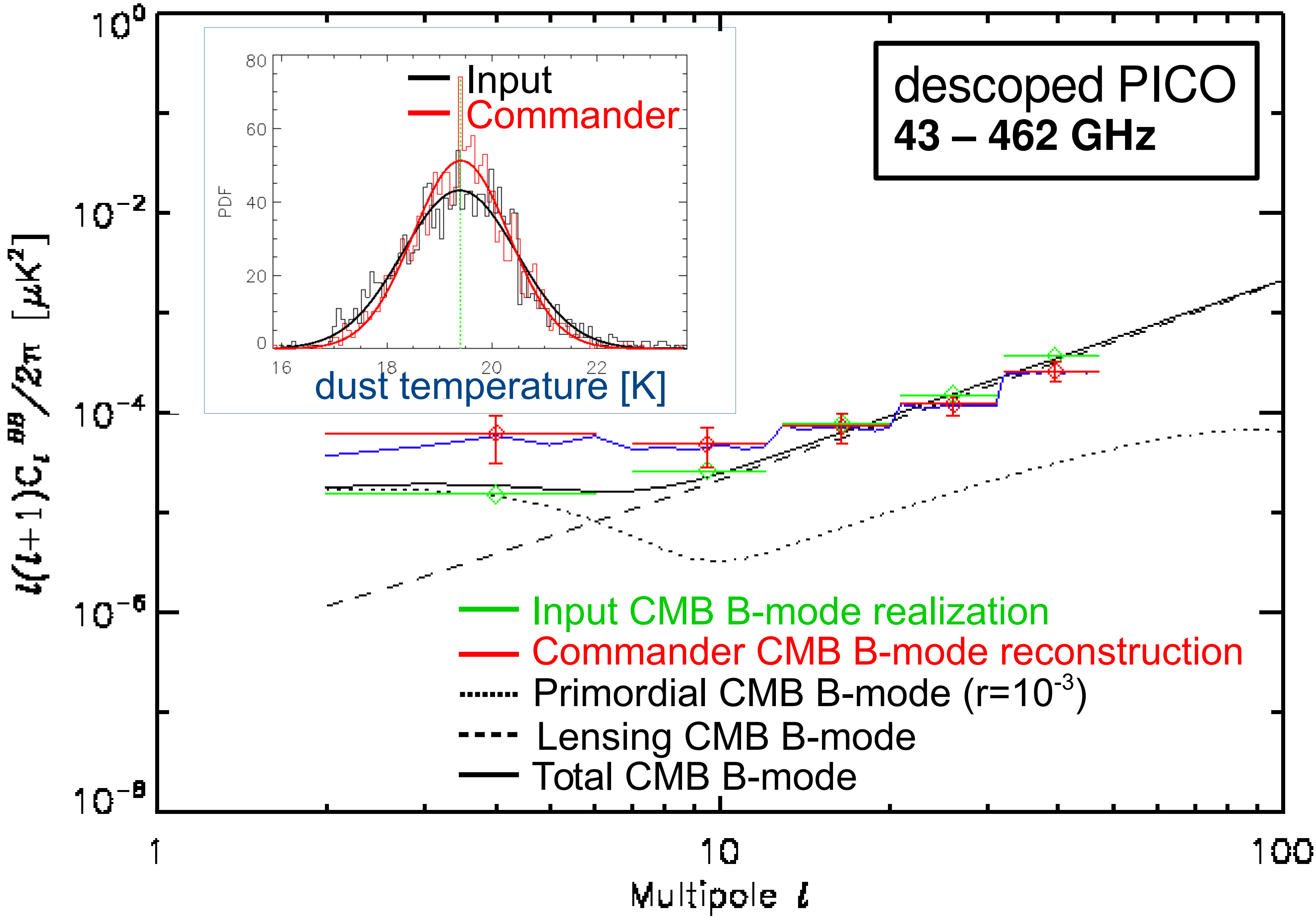

descoped PICO
43 – 462 GHz
Input
Commander
PDF
dust temperature [K]
Input CMB B-mode realization
Commander CMB B-mode reconstruction
Primordial CMB B-mode (r=10^-3)
Lensing CMB B-mode
Total CMB B-mode
Multipole ℓ
ℓ(ℓ+1)C_ℓ^BB/2π [μK^2]

Subtle issues for B-mode component separation

#1. Foreground mismodelling

Impact on r of mismodelling two MBB dust components as a single MBB component:

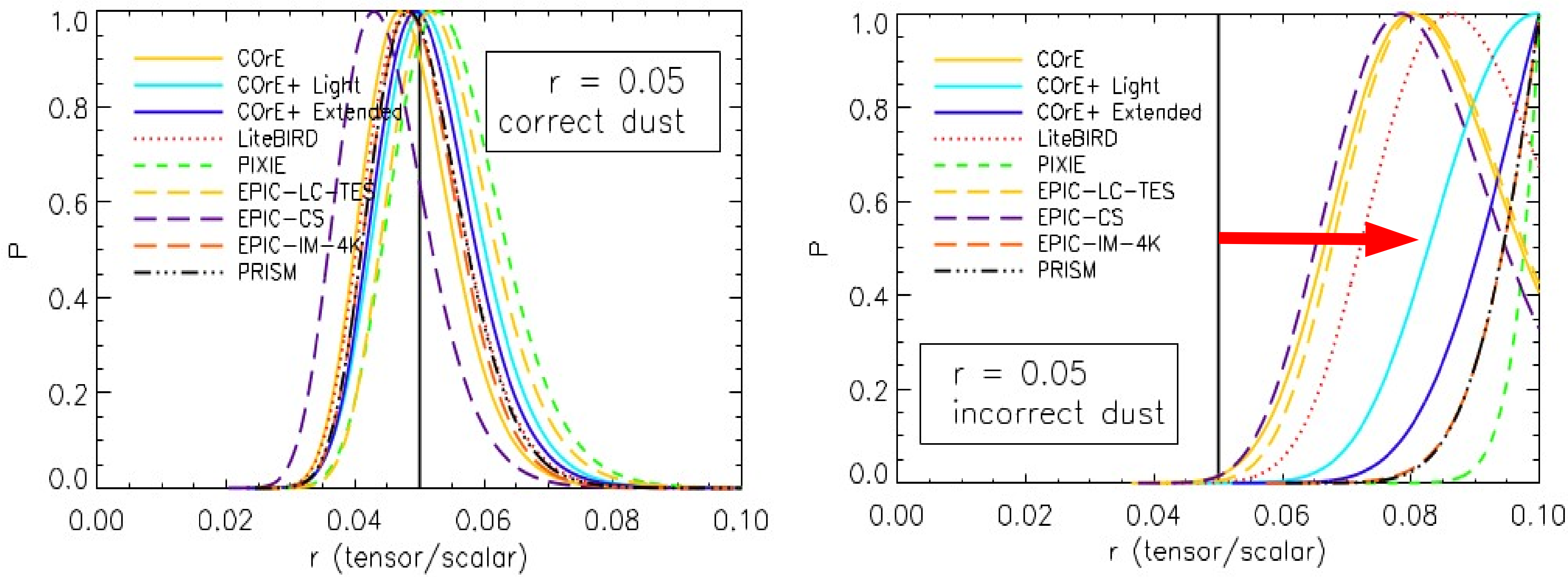

Remazeilles, Dickinson, Eriksen, Wehus, MNRAS (2016)

The Sneaky Point:

CMB experiments with narrow frequency range < 400 GHz show no evidence (χ2 ~ 1) for incorrect foreground modelling!

#2. Extragalactic compact foregrounds cannot be ignored

Polarized Radio and IR compact sources at ~ 100 GHz dominate the primordial CMB B-mode at $r = 10^{-3}$ on angular scales $\ell \gtrsim 50$

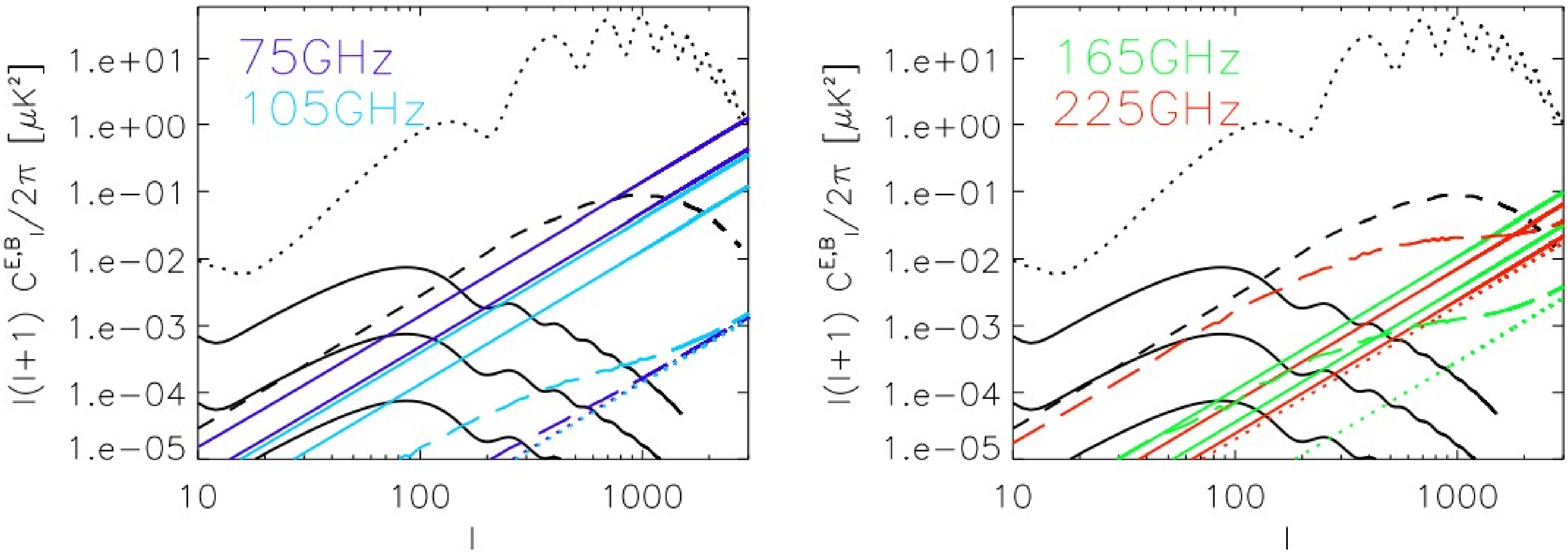

Curto et al 2013

#3. What about magnetic dust (MD)?

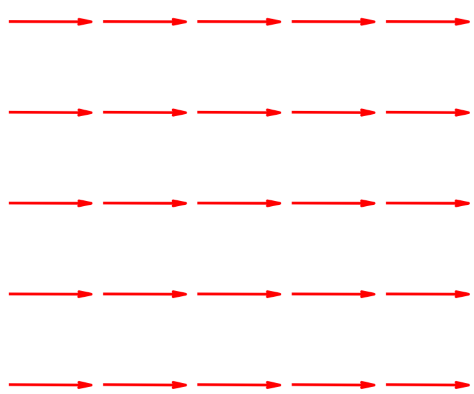

Ferromagnetic lattice with spins aligned.

Thermal fluctuations will move them away, producing magnetic dipole radiation

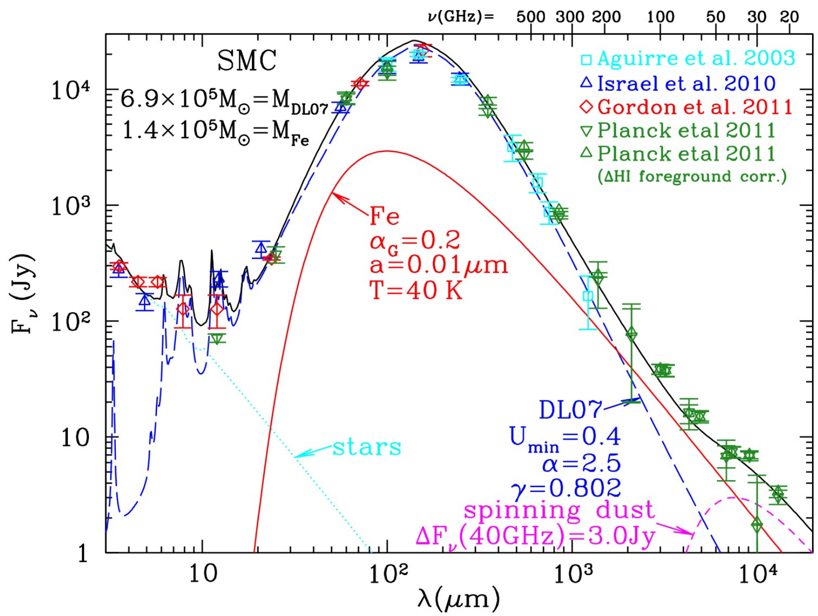

Draine & Hensley 2013

- **Diffuse MD not yet observed!**
- **In theory, MD might be highly polarized ~35%**
- **Spectral degeneracy at ~ 100 GHz between CMB and MD**

  → *can be a killer for component separation*

#4. Averaging effects

The actual foreground SED <u>on the maps</u> differs from the real SED <u>in the sky</u> !

Chluba, Hill, Abitbol, 2017

Dust spectral indices in the sky

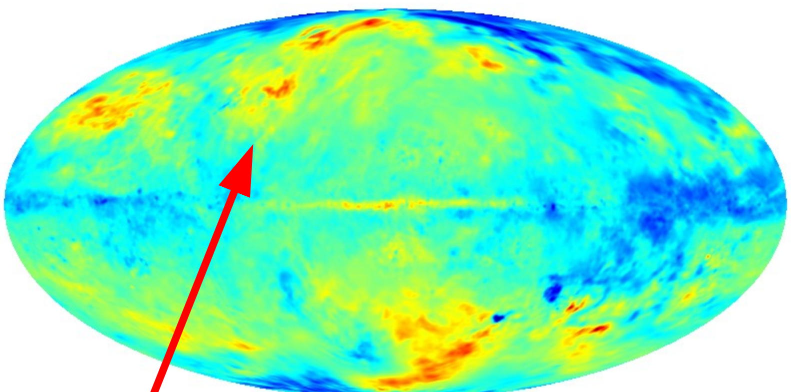

one value β_{dust} per line-of-sight

Mapping / pixelization

many values β_{dust} per pixel

(effective SED: $\sum_i \nu^{\beta i} = \nu^{\beta + C\,Log(\nu) + \dots}$)

Pixelization/averaging creates spurious curvatures on the foreground SED!

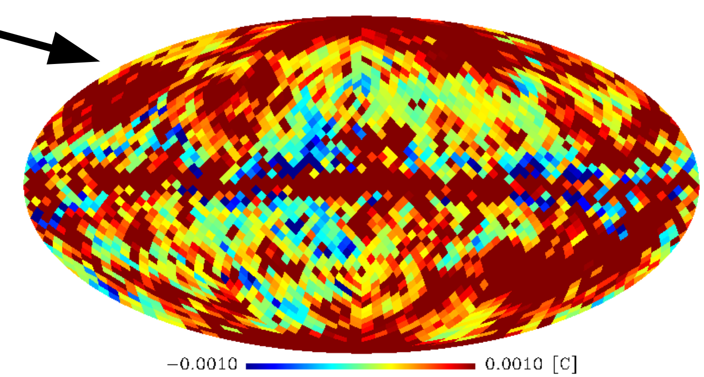

→ Bias of $\Delta r \approx 10^{-3}$ if ignored in the parametric fitting

Remazeilles et al 2017,
for the CORE collaboration

Alternative solutions: effective modelling?

Moment expansion of the full foreground SED:

$$(\nu/\nu_0)^{\beta}\,(1 + C_1\,(\ln(\nu/\nu_0))^2 + C_2\,(\ln(\nu/\nu_0))^3 + \dots)$$

Chluba, Hill, Abitbol, 2017

Moment expansion:
dust temperature vs curvature

MBB

$$(\nu/\nu_0)^{\beta}\, B(\nu, T)$$

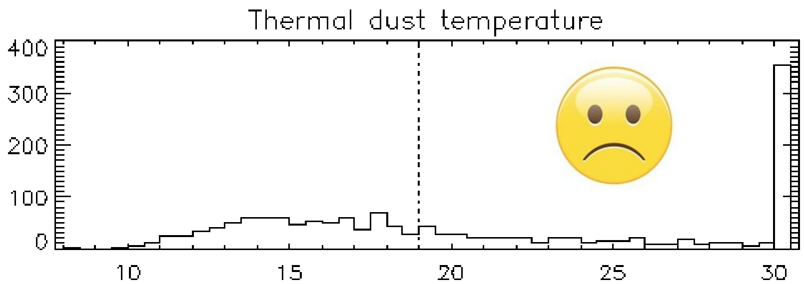

Curved power-law

$$(\nu/\nu_0)^{\beta}\,(1 + C\,(\ln\,(\nu/\nu_0))^2 + \ldots)$$

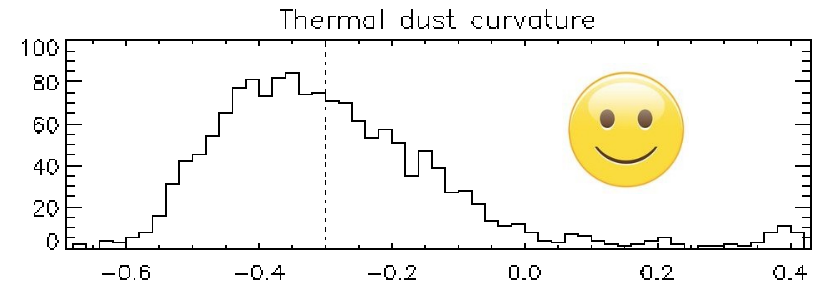

Example on LiteBIRD 40 – 402 GHz

Without frequencies > 400 GHz, dust temperature is not well constrained

Curvature is local thus better constrained than temperature over a narrow frequency range

M. Remazeilles

Conclusions

After foregrounds cleaning (COMMANDER + SMICA / NILC) and 60% delensing,

- CORE 60 – 600 GHz able to recover the primordial CMB B-mode power spectrum at $r = 5 \times 10^{-3}$ on both reionization and recombination peaks without bias.

- CORE 60 – 600 GHz able to detect $r = 5 \times 10^{-3}$ at 4σ significance without bias.
  → *allows to constrain the Starobinsky's R^2 inflation model.*

After foregrounds cleaning (COMMANDER),

- PICO 21 – 800 GHz able to detect $r = 10^{-3}$ at 2.5σ significance without bias.

- PICO 43 – 462 GHz (narrow frequency range) fails to detect $r = 10^{-3}$
→ *significant bias due to foreground contamination on large scales*

General issues that future CMB B-mode experiments will be facing:

- Foreground mismodelling: omitting curvature, AME, dust components, decorrelation
- Lack of frequency range / sensitivity to β_{synch} and T_{dust}
- Averaging effects of foreground SEDs by pixelization / beam convolution
- Spectral degeneracies, e.g. CMB and magnetic dust?

Alternative solutions: moment expansion (Chluba et al 2017)

Thanks for your attention!

Backup slides

Why a broad frequency range is essential?

- **To provide "lever arms" at low/high frequency for sensitive constraints on T_{dust} and β_{synch}**

  → *If not, then ~1% errors on T_{dust} and β_{synch} will extrapolate to an error $\Delta r \sim 10^{-3}$ on the B-mode power at CMB frequencies ~100 GHz*

  Remazeilles et al 2017, for the CORE collaboration

- **To provide "red flags" on incorrect foreground modelling/assumptions and χ2-evidence for false detections of r**

  → *Over a narrow frequency range, a multi-component fit can still get a good χ2 for the accurate fitting of the total sky emission (despite incorrect foreground models), nevertheless CMB and foreground B-modes might not be accurately separated!*

  Remazeilles, Dickinson, Eriksen, Wehus, MNRAS (2016)

- **To break spectral degeneracies:**

  → *At 70 – 100 GHz, the SEDs of CMB, magnetic dust, synchrotron with flattening curvature, are very much similar!*

  Draine & Hensley, ApJ (2013)
  Remazeilles, Dickinson, Eriksen, Wehus, MNRAS (2016)

COMMANDER

Methodology

Eriksen et al 2004, 2008
Remazeilles et al 2016, 2017

1. Component separation (Bayesian parametric fit with Gibbs sampler):

$$\boldsymbol{s}^{(i+1)} \leftarrow P\left(\boldsymbol{s}|C_\ell^{(i)}, \boldsymbol{\beta}^{(i)}, \boldsymbol{d}\right),$$ *amplitudes (CMB & foregrounds)*

$$C_\ell^{(i+1)} \leftarrow P\left(C_\ell|\boldsymbol{s}^{(i+1)}\right),$$ *power spectra (CMB)*

$$\boldsymbol{\beta}^{(i+1)} \leftarrow P\left(\boldsymbol{\beta}|\boldsymbol{s}^{(i+1)}, \boldsymbol{d}\right),$$ *spectral indices (foregrounds)*

2. Likelihood estimation of r and A_{lens}:

$$-2\ln\mathcal{L}\left[\widehat{C}_\ell|C_\ell^{th}\left(r, A_{lens}\right)\right] = \sum_\ell (2\ell+1)\left[\ln\left(\frac{C_\ell^{th}}{\widehat{C}_\ell}\right) + \frac{C_\ell^{th}}{\widehat{C}_\ell} - 1\right]$$

$$C_\ell^{th} = r\, C_\ell^{tensor}(r=1) + A_{lens}\, C_\ell^{lensing}(r=0).$$

3. Blackwell-Rao posterior:

$$\mathcal{P}\left(r, A_{lens}\right) \approx \frac{1}{N}\sum_{i=1}^{N}\mathcal{L}\left[\widehat{C}_\ell^i|C_\ell^{th}\left(r, A_{lens}\right)\right]$$

→ ***End-to-end propagation of the foreground uncertainties***

PICO reconstruction of primordial B-modes
No foregrounds, 50% mask

sample variance + noise
(50% of the sky)

r = 10^{-3} + lensing, f_{sky}=50%

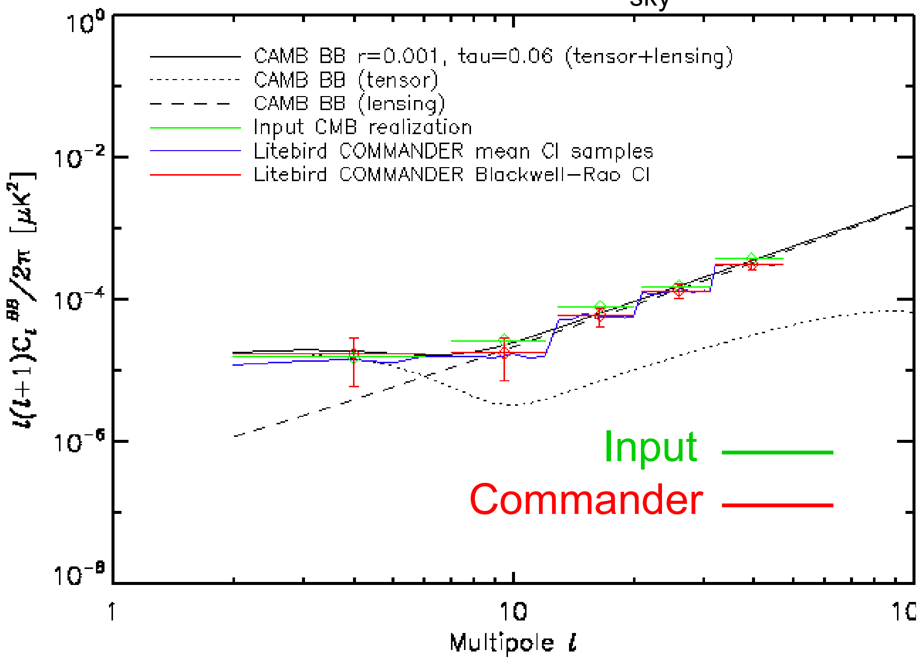

r = (0.6 ± 0.4) x 10^{-3}

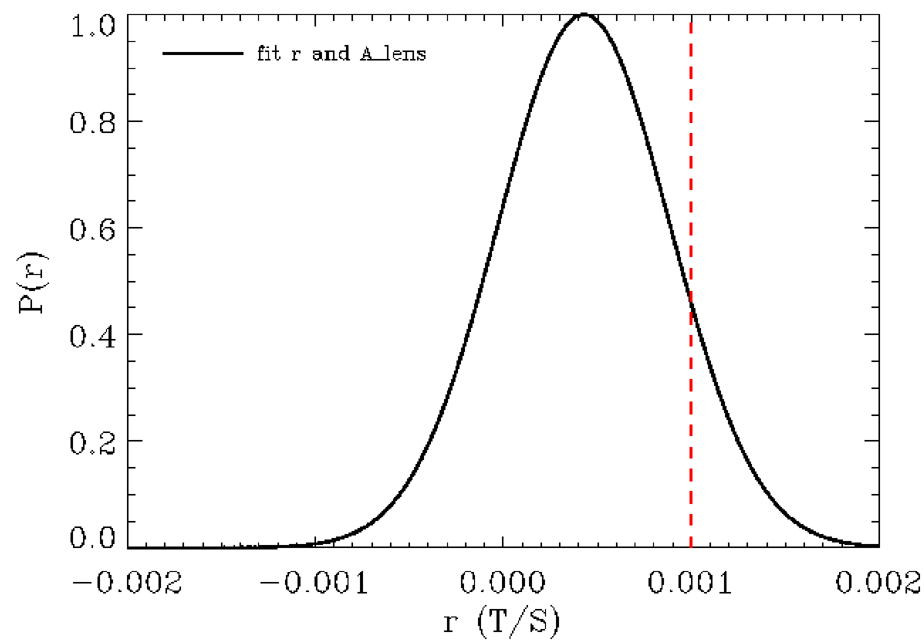

Sample variance σ(r = 10^{-3}) = 0.4 x 10^{-3}

That's the minimal uncertainty that can be achieved from 2 < ℓ < 50 <u>in the absence of foregrounds</u> on 50% of the sky

M. Remazeilles

Galactic foregrounds in polarization

Component	***Spectrum***	***Polarization fraction***	***References***
Synchrotron	*- Power-law $\beta \sim -3$, variations $\Delta\beta \sim 0.2$* *- In theory, curvature C=-0.3* *- Flattening from multiple power-laws / populations of electrons*	*~15-20%* *(up to ~50%)*	*Page et al (2007), Kogut et al (2007), Macellari et al (2011), Vidal et al (2015)*
Thermal dust	*- Modified black-body* *- Possibly 2 components/flattening at frequencies <300 GHz* *- Decorrelation across frequencies*	*~5% - 10%* *(up to ~20+%)*	*Ponthieu et al (2005), Planck intermediate results. XIX (2015), Planck intermediate results. L (2016)*
Magnetic dust?	*- Similar to thermal dust, but flatter index at frequencies ~100 GHz* *- Not yet detected (70GHz-300 GHz)*	*Variable* *(up to ~35% ?)* *<~5%*	*Draine & Lazarian (1999), Draine & Hensley (2013), Hoang & Lazarian (2015)*
Anomalous Microwave Emission (AME)	*- Peaked spectrum ~10-60 GHz*	*<~1%*	*Lazarian & Draine (2000), Dickinson (2011), Lopez-Caraballo et al. (2011), Macellari et al. (2011), Rubino-Martin et al. (2012), Planck 2015 results. XXV*
Free-free	*- Power-law $\beta \sim -2.14$ with positive curvature (steepening at frequencies >~100 GHz)*	*Intrisically zero,* *in practice <~1%*	*Rybicki & Lightman (1979), Keating et al. (1998), Macellari et al. (2011)*